Energy 317 (2025) 134678

Contents lists available at ScienceDirect

Energy

journal homepage: www.elsevier.com/locate/energy

Modeling a realistic integrated energy hub with growing demand for electric vehicles: The case of the province of Ontario, Canada

Ahmad Siroos *, Hamed Samarghandi

Edwards School of Business, University of Saskatchewan, Saskatoon, SK, Canada

ARTICLE INFO

Keywords:
Combined cooling
Heating and power
Energy hub
Electric vehicles
Information gap decision theory
Risk averse and risk seeker IGDT
Robust method

ABSTRACT

Energy hubs are multi-carrier energy management systems that efficiently distribute various forms of energy, reducing losses and environmental pollution. This paper examines Ontario, Canada, as a major energy hub, using a typical fall day pattern for energy demand. The model includes all power generation sources in Ontario: photovoltaic (PV), wind turbine (WT), nuclear, hydro, biofuel, and natural gas power plants. It also integrates the charging and discharging of electric vehicles (EVs) within the energy distribution framework.

Managing the intrinsic uncertainty of the parameters is crucial for efficient operation. This study employs probabilistic functions to account for the arrival and departure hours of EVs, controlled using the Conditional Value at Risk (CVaR) method. Three methods, Information Gap Decision Theory (IGDT) with risk-seeking and risk-averse behaviors, and robust optimization, address uncertainties such as wind and solar electricity production, energy prices, and electrical, heating, and cooling demands.

We compare simulation results of three scheduling scenarios for optimal energy production and dispatch. The RS-IGDT method can lead to significant losses during peak hours due to fluctuations. The robust method incurs higher costs by planning for large deviations. The RA-IGDT method balances deviations without the pessimism of the robust method, making it the recommended approach.

Nomenclature

Sets			
t	Time of day which includes 24 h	j	Set of random simulations for EVs
i	Set of EVs		
Parameters			
OM_{Nuc}	The O&M cost per unit of nuclear power generated	DR^{E}_{up}	Cost per unit of upward regulation of the electrical DRP
OM_{Hyd}	The O&M cost per unit of generated power in the hydro power plant	DR^{E}_{down}	Cost per unit of downward regulation of the electrical DRP
OM_{Bio}	The O&M cost per unit of generated power in the biofuel power plant	DR^{H}_{up}	Cost per unit of upward regulation of the heat DRP
OM_{Gas}	The O&M cost per unit of generated power in the gas power plant	DR^{H}_{down}	Cost per unit of downward regulation of the heat DRP
OM_{PV}	The O&M cost per unit of generated power in the solar power plant	DR^{C}_{up}	Cost per unit of upward regulation of the cooling DRP

(*continued on next column*)

(*continued*)

Sets			
OM_{WT}	The O&M cost per unit of generated power in the WT power plant	DR^{C}_{down}	Cost per unit of downward regulation of the cooling DRP
OM_{GT}	The O&M cost per unit of generated energy in the gas turbine	MR^{E}_{up}	Maximum ratio of shifted up electrical demand
OM_{GB}	The O&M cost per unit of generated energy in the gas boiler	MR^{E}_{down}	Maximum ratio of shifted down electrical demand
OM_{EC}	The O&M cost per unit of consumed power in the electric chiller	MR^{H}_{up}	Maximum ratio of shifted up heat demand
OM_{AC}	The O&M cost per unit of consumed heat in the absorption chiller	MR^{H}_{down}	Maximum ratio of shifted down heat demand
OM_{ISC}	The O&M cost per unit of consumed power in the ice storage conditioner	MR^{C}_{up}	Maximum ratio of shifted up cooling demand

(*continued on next page*)

* Corresponding author.
E-mail address: ahmadsiroos@yahoo.com (A. Siroos).

https://doi.org/10.1016/j.energy.2025.134678
Received 27 September 2024; Received in revised form 15 January 2025; Accepted 20 January 2025
Available online 26 January 2025

(*continued*)

Sets			
OM_{HS}	The O&M cost per unit of stored heat in the heat storage unit	MR^{C}_{down}	Maximum ratio of shifted down cooling demand
EM_{Nuc}	The emission cost per unit of power generated in the nuclear power plant	η^{EV}_{ch}	EV charging efficiency
EM_{Hyd}	The emission cost per unit of power generated in the hydro power plant	η^{EV}_{dch}	EV discharging efficiency
EM_{Bio}	The emission cost per unit of power generated in the biofuel power plant	$E^{EV}_{min,j}$	Minimum required electrical charge of the j-th EV
EM_{Gas}	The emission cost per unit of power generated in natural gas power plant	$E^{EV}_{max,j}$	Capacity of the battery of the j-th EV
EM_{PV}	The emission cost per unit of power generated in the solar power plant	$P^{EV}_{ch,max,j}$	The maximum amount the j-th EV can be charged in 1 h
EM_{WT}	The emission cost per unit of power generated in the wind turbine power plant	$P^{EV}_{dch,max,j}$	The maximum amount the j-th EV can contribute to the hub in 1 h
EM_{GT}	The emission cost per unit of generated energy in the gas turbine	$P^{EV}_{ch,max}$	The maximum allowed amount that all EVs can be charged in 1 h
EM_{GB}	The emission cost per unit of generated energy in the gas boiler	$P^{EV}_{dch,max}$	The maximum allowed amount that all EVs can contribute to the hub in 1 h
Rep^{EV}_{j}	Cost of replacing the battery for j-th EV	Cap^{EV}_{j}	Total capacity of the battery of the j-th EV during its entire lifetime
Pr^{e}_{t}	Price factor for buying electricity	G^{GB}_{max}	Maximum allowable limit of natural gas for GB unit
λ^{G}_{t}	Price of natural gas in period t	H_{max}	Maximum produced heating energy
η^{HS}_{ch}	Heat storage charging efficiency	P^{L}_{t}	Electrical demand
η^{HS}_{dch}	Heat storage discharging efficiency	H^{L}_{t}	Heat demand
E^{HS}_{min}	Minimum limit of heat stored energy in HS unit	C^{L}_{t}	Cooling demand
E^{HS}_{max}	Maximum limit of heat stored energy in HS unit	V_{Gas}	Low calorific value of natural gas
$H^{HS}_{ch,max}$	Maximum limit of charging heating energy in an hour for HS unit	η_{GB}	Efficiency of GB
$H^{HS}_{dch,max}$	Maximum limit of discharging heating energy in an hour for HS unit	η^{e}_{GT}	Electrical efficiency of GT
η^{ISC}_{ch}	ISC charging efficiency	η^{h}_{GT}	Heating efficiency of GT
η^{ISC}_{dch}	ISC discharging efficiency	β_t	degree of the uncertainty in period t
COP_{EC}	Coefficient of performance for electric chiller	ω	The deviation factor of total casts in the IGDT method
COP_{AC}	Coefficient of performance for absorption chiller	$\widehat{Pr}^{e}_{t}$	The lower bound of Price coefficient for buying electricity from the grid
COP_{ISC}	Coefficient of performance for ISC	$\widehat{P}^{PV}_{t}$	The lower bound of electric power produced by PV
E^{ISC}_{min}	Minimum limit of stored cooling energy for ISC unit	$\widehat{P}^{WT}_{t}$	The lower bound of electric power produced by WT
E^{ISC}_{max}	Maximum limit of stored cooling energy for ISC unit	$\widehat{P}^{L}_{t}$	The upper bound of electrical power demand
$P^{ISC}_{t,max}$	Maximum limit of charging electrical power in an hour for ISC unit	$\widehat{H}^{L}_{t}$	The upper bound of heating energy demand
$C^{ISC}_{t,max}$	Maximum limit of discharging cooling energy in an hour for ISC unit	$\widehat{C}^{L}_{t}$	The upper bound of cooling energy demand
G^{GT}_{max}	Maximum allowable limit of natural gas for GT unit		
Main variables			
OF	Objective function	G^{GB}_{t}	Consumed gas from the gas boiler in period t
$Cost_{OM}$	Total O&M cost of all units	H^{GB}_{t}	Heat energy generated by the gas boiler in period t

(*continued on next column*)

(*continued*)

Sets			
$Cost_{EM}$	Total emission cost of all units	P^{EC}_{t}	Electric power generated by the electric chiller in period t
$Cost_{Bat}$	Total battery cost of all EVs	H^{AC}_{t}	Electric power generated by the absorption chiller in period t
$Cost_{DR}$	Total cost related to DRP	P^{ISC}_{t}	Electric power discharged from the ISC in period t
$Cost^{PP}_{OM}$	Total O&M cost of all power plants	$H^{HS}_{dch,t}$	Heat energy discharged from the heat storage unit in period t
$Cost^{GT}_{OM}$	Total O&M cost of the gas turbine	$H^{HS}_{ch,t}$	Heat energy charged for the heat storage unit in period t
$Cost^{GB}_{OM}$	Total O&M cost of the gas boiler	$P^{EV}_{ch,j,t}$	Electric power charged for the j-th EV in period t
$Cost^{EC}_{OM}$	Total O&M cost of the electric chiller	$P^{EV}_{dch,j,t}$	Electric power discharged from the j-th EV in period t
$Cost^{AC}_{OM}$	Total O&M cost of the absorption chiller	P^{up}_{t}	Increased power by DRP in period t
$Cost^{ISC}_{OM}$	Total O&M cost of the electric chiller	P^{down}_{t}	Decreased power by DRP in period t
$Cost^{HS}_{OM}$	Total O&M cost of the heat storage unit	H^{up}_{t}	Increased heat energy by DRP in period t
$Cost^{PP}_{EM}$	Total emission costs of all power plants	H^{down}_{t}	Decreased heat energy by DRP in period t
$Cost^{GT}_{EM}$	Total emission costs of the gas turbine	C^{up}_{t}	Increased cooling energy by DRP in period t
$Cost^{GB}_{EM}$	Total emission costs of the gas boiler	C^{down}_{t}	Decreased cooling energy by DRP in period t
P^{Nuc}_{t}	Electric power generated by the nuclear power plant in the period t	$E^{EV}_{j,t}$	Electric energy stored by the j-th EV in period t
P^{Hyd}_{t}	Electric power generated by the hydroelectric power plant in the period t	$t_{arr,j}$	The arrival time of the j-th EV
P^{Bio}_{t}	Electric power generated by the biofuel power plant in the period t	$t_{dep,j}$	The departure time of the j-th EV
P^{Gas}_{t}	Electric power generated by the gas power plant in period t	E^{HS}_{t}	Heat energy stored by the heat storage unit
P^{PV}_{t}	Electric power generated by the solar power plant in period t	P^{ISC}_{t}	Consumed electric power by the ISC in period t
P^{WT}_{t}	Electric power generated by the wind turbine in period t	P^{PP}_{t}	Total Electric power generated by all power plants in period t
G^{GT}_{t}	Consumed gas by the gas turbine in period t	C^{EC}_{t}	Cooling energy generated by the electric chiller in period t
P^{GT}_{t}	Electric power generated by the gas turbine in period t	C^{AC}_{t}	Cooling energy generated by the absorption chiller in period t
H^{GT}_{t}	Heat energy generated by the gas turbine in period t		
Binary variables			
$I^{E.up}_{t}$	Indicator for increasing electric demand in period t	$Z^{ch}_{j,t}$	Indicator for charging the j-th EV in period t
$I^{E.down}_{t}$	Indicator for decreasing electric demand in period t	$Z^{dch}_{j,t}$	Indicator for discharging the j-th EV in period t
$I^{H.up}_{t}$	Indicator for increasing heat demand in period t	K^{ch}_{t}	Indicator for charging the heat storage unit in period t
$I^{H.down}_{t}$	Indicator for decreasing heat demand in period t	K^{dch}_{t}	Indicator for discharging the heat storage unit in period t
$I^{C.up}_{t}$	Indicator for increasing cooling demand in period t	N^{ch}_{t}	Indicator for charging the ISC in period t
$I^{C.down}_{t}$	Indicator for decreasing cooling demand in period t	N^{dch}_{t}	Indicator for discharging the ISC in period t
Abbreviations			
AC	Absorption Chiller	IGDT	Information Gap Decision Theory
CCHP	Combined Cooling, Heat, and Power	ISC	Ice Storage Conditioner
CVaR	Conditional Value at Risk	LHS	Latin Hypercube Sampling
DR	Demand Response	MG	Micro grid

(*continued on next page*)

(*continued*)

Sets			
DRP	Demand Response Program	O&M	Operation and Maintenance
EC	Electric Chiller	PV	Photovoltaic
EH	Energy Hub	RA-IGDT	Risk Averse-IGDT
EV	Electric Vehicle	RS-IGDT	Risk Seeker-IGDT
GB	Gas Boiler	SWD	Seawater Desalination
GT	Gas Turbine	V2G	Vehicle-to-Grid
HS	Heat Storage	WT	Wind Turbine

1. Introduction

As human societies develop, new industries and needs emerge. Their energy supply and consumption necessitate the creation of equipment and infrastructure for electricity production and transmission [1]. With the proliferation of distributed energy resources, the growing demand for electrical, thermal, and cooling energy, and the increasing pollution of energy carriers, Energy Hubs (EH) have become integral components of power system structures [2]. An EH is a multi-generation system that encompasses various energy sources (both renewable and non-renewable), diverse energy demands, and different storage units and energy converters. Consequently, the attention to energy hubs has been growing among researchers in recent years [3]. Studying energy production and consumption in the context of an Energy Hub (EH) creates advantages such as optimal utilization of installed capacity and environmental potential while meeting other common requirements like electricity, cooling, and heating. In addition, an EH can enhance its flexibility by converting energy into different forms, such as electrical, thermal, and cooling energy, and storing it [4].

On the other hand, the growing focus on air pollution has resulted in the widespread adoption of electric vehicles (EVs) and the utilization of hydrogen as an environmentally friendly fuel source. In recent years, with the increase in the number of EVs, the development of fast charging capabilities, and the increase in the capacity of batteries, there is an intensified need for their energy supply. The charging stations are increasing daily, further expanding the uncertainty for this type of load [5]. In recent years, researchers have considered the possibility of using EV batteries as a form of storage of electric energy, which is addressed as Vehicle-to-Grid (V2G) in the literature. In this case, the charging stations are designed such that they allow both charging EV batteries and the release of stored energy to respond to the network's needs during peak demand periods [6].

In this case, modeling the electric network as an energy hub not only coordinates the required load and optimizes the uncertainty of operating charging stations, but also minimizes the costs of the power system [7]. There are other uncertainties in an energy hub, which further complicate decision-making. The demands for electrical, thermal, and cooling loads are among the most important sources of uncertainty and have the greatest impact on the uncertainty of the system [8]. EHs usually consist of renewable and non-renewable energy production sources, where the amount of energy produced through renewable sources such as PV and WT is uncertain. These sources of uncertainty must be carefully considered in such an EH to avoid substantial financial losses [9].

In this paper, a large-scale real-world energy hub, which is the province of Ontario in Canada, is studied during 24 h of its operation. Electrical, thermal, and cooling energy demands are included in the considered hub and optimal load distribution is calculated simultaneously for all the three categories. The role of electric vehicles, with both consumption and storage functionalities, is examined in detail as one of the main parts of the energy hub. The CVaR method is employed to deal with the uncertainty caused by the inclusion of EVs. The other major sources of uncertainty considered in this article are the electric, thermal, and cooling energy demands, energy prices at different times of the day, and the amount of power produced by wind and solar power plants. Three methods, namely Robust, RA-IGDT, and RS-IGDT methods, are employed to handle the uncertain parameters. A thorough numerical analysis is performed to compare these methods and managerial insights are provided.

The rest of this paper is organized as follows. Section 2 reviews the related literature and discusses the novelties of this paper. Section 3 presents the structure of the studied energy hub. Section 4 models the energy hub and introduces the methods of solving the resulted optimization problem. Section 5 discusses the simulation results and the numerical analysis. Section 6 concludes the paper and debates future research directions.

2. Literature review

With the ongoing rise in pollution and greenhouse gases, a prudent approach to addressing this issue involves developing methods to utilize energy to achieve a more stable grid and reduce greenhouse gas emissions. Incorporating EVs powered by renewable energy sources can serve as a solution or, at the very least, a suitable strategy to mitigate these challenges [10]. Creating appropriate platforms, such as promoting the adoption of vehicle-to-grid EVs, can enhance stability within smart networks, an integrated system that manages multiple forms of energy (such as electricity, heat, and gas) and their interconversion, distribution, and consumption in an optimized and coordinated manner [11]. Therefore, the adoption of EVs should be accompanied by infrastructure improvements in telecommunications and control. Neglecting the intelligence of the electrical grid infrastructure could render EVs less efficient and beneficial [12]. The combined use of EVs and renewable energies can contribute to a smoother energy generation profile. Consequently, it has become customary to implement energy systems that support multiple energy models simultaneously, including refrigeration systems for combined heat and power generation [13]. The emphasis on this point involves viewing EVs as mobile storage units capable of storing energy and injecting it into the grid when necessary [14].

2.1. The concept of energy hubs

[15] optimized the layout for a multi-carrier energy hub that includes battery energy storage systems. The goal was to meet the energy needs of the hub and effectively manage the flow of energy. The suggested model considered several energy sources, such as thermal energy, natural gas, and electricity, while also taking into account cost and operational restrictions [16]. concentrated on using reinforcement learning techniques to maximize the efficiency of an EH within the framework of smart grids to address the problems related to effective energy management in intricate systems. By use of these methods, EHs can adjust their operational choices in response to feedback from the network, user preferences, and external factors [17]. covered the usage of mathematical programming with equilibrium constraints to analyze the role of an energy hub in the markets for the distribution of heat and electricity. The main objective was to maximize the participation of the energy hub in the heat and power markets through energy management.

[18] aimed to develop a strategy to maximize the use of distributed energy hubs with several goals such as lowering costs, increasing energy efficiency, and minimizing the environmental effects. This research illustrated the efficacy of the developed strategy to achieve optimal EH operations and emphasized the need to consider a variety of goals and trade-offs when developing energy management plans for dispersed energy hubs to guarantee effective and sustainable energy systems [19]. focused on energy management and optimized the performance of a smart multi-energy hub system and presented a framework to combine demand response tactics with energy hub coordination. This framework which incorporated demand response techniques allowed for dynamic management of energy supply and demand, which improved flexibility and lowered operating costs.

2.2. Managing uncertainty in energy hubs

Energy systems frequently involve uncertainty; modeling and managing this uncertainty is essential to maximizing the efficiency of energy hubs. Decision-makers can acquire insight into the possible risks that affect system performance by integrating uncertainty into energy hub models. The intuitions obtained lead to the creation of resilient and adaptable operating plans that reduce the effects of uncertainty and adapt to changing circumstances. The shift to efficient and sustainable energy systems is largely dependent on energy hubs that combine various energy sources and technologies [20]. However, achieving reliable and economical exploitation is severely hampered by the inherent unpredictability and instability of renewable energy sources, energy demand, and market circumstances [21]. As a result, research on uncertainty modeling in energy hubs has become increasingly important.

In an energy hub, decisions related to energy production, distribution, and storage are heavily influenced by several key factors: the price of energy production, the demand for different types of energy, the amount of energy produced by renewable sources, the charging requirements of electric vehicles, and the capacity of electric vehicles to inject energy back into the power grid. These factors are typically beyond the control of energy hub operators. While operators can influence these parameters through strategies such as dynamic pricing and demand response programs, the exact values are difficult to forecast due to unpredictable elements such as weather conditions, consumer behavior, and regulatory changes. This uncertainty complicates the energy hub's ability to estimate precise values for energy demand, supply costs, and renewable energy output. Therefore, decision-makers need to account for this uncertainty while creating models that accurately represent realistic scenarios. Common methods used to manage these uncertainties in energy hubs include stochastic optimization, fuzzy set theory, robust optimization (RO), RA-IGDT, RS-IGDT, and CVaR [22].

In energy planning, many studies address uncertain parameters through the use of stochastic or fuzzy programming. Nevertheless, accurately determining the probability distribution of uncertain parameters, such as energy prices or renewable output, remains a significant challenge. This difficulty is compounded by the often-sparse historical data, which might result in incorrect outcomes. Although stochastic programming can provide parameter values that are probable to be correct, there is always a chance that these estimates could be incorrect, potentially rendering solutions infeasible and resulting in significant cost increases. Despite the high accuracy of stochastic programming, the associated risk must be carefully managed when making decisions in an energy hub context [23].

Similarly, fuzzy set theory presents its own challenges, as it requires extensive knowledge and understanding of the parameters to generate accurate membership functions. Gaining such comprehensive knowledge about the energy market dynamics, including electric vehicle behaviors and renewable energy variability, poses a significant challenge for decision-makers and limits the effective use of fuzzy set theory for real-world optimization problems [24].

Robust optimization is an analytical method specifically developed to handle uncertainty in decision-making and has fewer disadvantages when compared to the aforementioned techniques. Both robust and stochastic optimization utilize past data to forecast scenarios and probability distributions. When these predictions are accurate, they can effectively reflect the uncertain characteristics of variables like energy demand and production costs [25]. However, the accuracy of these predictions depends on the volume of data and the precision of the methods used; inaccuracies can lead to heightened intricacy and diminished certainty. Robust optimization involves representing uncertain parameters as members of an uncertainty set, which can be specified in various ways, such as bounded sets or sets of scenarios. The aim of robust optimization is to find decisions or solutions that perform well under the worst-case scenarios within the given uncertainty set, ensuring optimal solutions with good generalization and manageable complexity [7].

Robust optimization considers various scenarios as possible outcomes, assigning a probability of occurrence to each. The objective is to obtain solutions that are nearly optimal and feasible across these scenarios. Historical data is still used to determine the likelihood of each scenario, but robust optimization addresses potential infeasibility by incorporating the cost of infeasibility into the model [4].

Stochastic programming aims to maximize the expected value of the objective function across all possible scenarios, while robust optimization generates solutions that are feasible for all scenarios and treats infeasibility as a cost. Although determining the correct probability of scenario occurrences remains a challenge for robust optimization, it is mitigated by factoring in the cost of infeasibility. In stochastic models, incorrect parameter predictions can lead to infeasible solutions, higher costs, and reduced effectiveness of decision support systems. However, robust optimization inherently considers infeasibility costs, delivering a single optimal solution feasible across all scenarios [26].

Information Gap Decision Theory (IGDT) provides another method for managing uncertainty, focusing on risk-averse (RA-IGDT) and risk-seeker (RS-IGDT) strategies. RA-IGDT aims to find solutions that are robust against worst-case scenarios of uncertain parameters, minimizing performance risk. Conversely, RS-IGDT seeks solutions that can capitalize on the best-case scenarios, maximizing potential benefits [3].

Conditional Value at Risk (CVaR) focuses on managing the risk of extreme events, measuring the expected value of the objective function in the worst-case percentile of outcome distributions. This method is particularly useful in energy hubs, where extreme events such as sudden spikes in energy demand, fluctuations in renewable energy production, or unexpected electric vehicle charging patterns can significantly impact operations [27].

By employing these methods, energy hubs can better manage the inherent uncertainties in their operations, leading to more reliable and cost-effective energy production, distribution, and storage. Interested reader is referred to Ref. [28] to learn more about methods of addressing uncertainty in an optimization model.

[29] introduced an adaptable **robust** optimization strategy to handle uncertainty in the two-stage operation of EH-based microgrids. The column-and-constraint generation (C&CG) process, which splits the framework into a master problem and a sub-problem, was used to linearize and solve the suggested model. The sub-problem used a max-min objective function to compute the dispatch cost associated with the worst realization of uncertainty, while the master problem minimized the unit commitment cost. This study aimed to address uncertainty-related issues such as demand load, power prices, and renewable energy production, and proposed an adjustable set of parameters to allow robust decision-making at a range of uncertainty levels [30]. demonstrated a risk-averse planning strategy for an energy hub with uncertain variables, which aimed to improve the performance of the hub while accounting for the variability in renewable energy production, electricity prices, and demand load, considering the time of use (TOU) and real-time pricing (RTP) for load management schedules. A scenario-based method was used to simulate uncertainties, while correlations between unknown variables were handled by a **robust** optimization strategy.

[31] developed a **stochastic** optimization model of an energy hub which included demand response and thermal energy market, where the sources of uncertainty were demand load, electricity cost, and the amount of renewable energy production. The proposed approach encouraged energy trading and adjustment of operations in response to market conditions and demand for thermal energy to meet both thermal and electrical needs while minimizing the operational costs of the hub [32]. examined the stable condition of a price-making EH, an area or platform where energy prices are set by gathering and trading energy commodities including oil, natural gas, and electricity, in a competitive

market with focus on price uncertainty and its effects on the hub's decision-making process. By serving as focal points for energy supply and demand, price-making hubs set benchmark prices that affect local, national, and even international markets [32]. used **game theory** to analyze the interplay between market participants. Additionally, they used **stochastic processes** to model the uncertainty in electricity pricing, considering both the mean and the covariance matrix of price movements.

[33] studied energy management in adaptable EHs connected to the grid by creating a network that included both heating and electricity, where the hub, which involved renewable energy sources and storage devices, acted as a central coordinator. Their proposed model considered uncertainties regarding demand, cost of heating and electrical energy, and renewable power sources [34]. described the management of energy in electrical and thermal networks with variable pricing schemes and integrated renewable energy hubs to improve network flexibility. The hub included renewable energy sources such as biofuel units, energy storage, and responsive loads. They suggested a plan to reduce the difference between the energy cost of the network and the flexibility of the hub, governed by the hub flexibility model, operation model of resources, storage, and responsive loads.

[35] designed a hybrid renewable energy system with wind turbines and biofuel energy units combined with stationary (batteries) and mobile (electric cars) energy storage and employed the **IGDT method** to deal with uncertainties.

A network of dispersed, medium-sized power generating units, such as wind farms, solar panels, and combined heat and power units, along with flexible power consumers and storage systems, integrated to operate as a single power plant is known as a virtual power plant or VPP. VPPs can provide their pooled energy production and flexibility services to participate in energy markets, especially those run by energy hubs. Energy hubs and VPPs are two cutting-edge strategies for updating the energy infrastructure. VPPs introduce decentralized, flexible generation and consumption into the market, facilitating the shift toward a more robust and sustainable energy system, while energy hubs concentrate on centralized trade and price-setting. In the context of flood and earthquake events [36], highlighted the robust performance of a smart distribution network in view of flexible renewable VPPs with the goal of reducing the overall cost of the smart distribution network. The model included resiliency constraints, virtual power plant constraints, and AC optimum power flow equations.

[13] presented a novel optimization model to achieve flexible-reliable operation (FRO) of EHs in networks for district heating, natural gas, and electricity. The proposed model used Energy storage technologies and a demand response program based on incentives to increase the flexibility of energy hubs in the context of combined heat and power systems and renewable energy sources.

There are studies that consider seawater desalination (SWD) considering the thermal and electrical energy requirements of SWD combined with other cooling and heating demands (CCHP). For example [37], studied an effective and reliable complex system that meets energy and freshwater demands in the presence of renewable energy sources. Numerous studies have explored the utilization of CCHP and/or renewable energy sources alongside SWD in both grid-connected and island microgrids, with a foundation in energy harvesting. For instance Ref. [38], devised an optimal plan for a grid-connected microgrid that integrates CCHP, CSP, BESS, TESS, and SWD to reduce investment and operational expenses. Similarly [24], optimized an isolated energy hub, relying on WT, CSP, and SWD to minimize overall system costs without exchanging energy with the main grid [39]. introduced an algorithm called the leader–follower optimization method for the optimal design and operation of microgrids equipped with SWD systems. However, neither [24,38,39] considered the unpredictable variability inherent in renewable energy generation and demand patterns.

2.3. Research gaps

One can confirm that in previous research efforts the details of power plants, which are considered as the main element in the power grid, have never been discussed. In each power grid, there are different types of power plants with their own characteristics in terms of cost and pollution.

Undoubtedly, considering these differences in the models has an immense effect on the overall cost and environmental impact of the energy hub. Some researchers assume that the energy hub is connected to the grid without discussing the elements and components of the electricity production of the grid. Furthermore, researchers who have viewed the energy hub as an isolated entity have not addressed the topic of power plants at all.

Another major gap in this research field is the lack of comparison of different approaches of dealing with uncertainty. Most articles that model uncertainty in the context of energy hubs employ a specific technique to handle uncertainty without presenting or comparing their results with other methods. Unfortunately, this lack of comparison leaves questions about the effectiveness of the various procedures unanswered.

Table 1 provides an overview of recent studies related to the topic of energy hubs. Additionally, this table highlights the unique aspects of the current work compared to other studies.

2.4. Contributions

This research focuses on the province of Ontario in Canada and includes all types of power plants that exist in Ontario and their maximum power production capacity in its modeling. Additionally, the costs of producing electricity and polluting the environment for each type of power plant are considered in the model. The impact of charging and discharging electric vehicles along with an analysis of the impact of the number of EVs in the hub has been incorporated into the paper. Consequently, this paper investigates the effect of increasing the number of electric vehicles on their participation in the V2G project.

This paper covers a comprehensive hub that includes electrical, thermal, and cooling energy consumptions. Afterward, a detailed definition and modeling of the system components are provided. The primary components consist of PV, WT, CCHP (Combined Cooling, Heating, and Power), thermal storage units, EV parking facilities, and electrical, thermal, and cooling energy demands. The system considers EV parking as a fundamental component, and thoroughly discusses its participation in electric energy hubs as both a consumer and a storage unit. This system accounts for individual sources and their inherent uncertainties. The Conditional Value at Risk (CVaR) method is used to contrast the uncertainty of electric vehicle issues. Three approaches are employed, namely, Risk-Seeking Information Gap Decision Theory (RS-IGDT), Risk-Averse IGDT (RA-IGDT), and the robust method, to model and optimize the system. This study integrates three advanced methods, RS-IGDT, RA-IGDT, and Robust Optimization, to address uncertainties in wind and solar electricity production, energy prices, and electrical, heating, and cooling demands, allowing a comparative analysis of their effectiveness. Additionally, the CVaR method is applied exclusively to EV-related uncertainties, providing a focused solution to charging and discharging variability. This combination of comprehensive modeling and methodical analysis contributes to both theoretical and practical advancements in energy hub optimization. The main contributions of this article include.

1. Presenting a comprehensive EH model that includes detailed information on all generating resources from the province of Ontario's grid.
2. Comparing the characteristics and effectiveness of three different approaches—RS-IGDT, RA-IGDT, and robust methods—of addressing uncertainty.

Table 1
Recent studies on energy hub scheduling.

Reference	Uncertainty modeling	Source of uncertainty	Detailed analysis of EVs	Objective function	Detailed grid	Demand types	Type of the model	Case study
[2]	–	–	–	Cost & emission	–	Power & heating & cooling	Stochastic	–
[25]	Robust	Demand	✓	Cost & emission	–	Power & heating	Stochastic	–
[37]	Fuzzy	Demand	–	Cost	–	Power & desalination	Deterministic	Canary Islands, Spain
[38]	Robust	PV & WT	–	Cost	–	Power & desalination	Stochastic	Astypalaia Island, Greece
[40]	–	–	–	Cost	–	Power & heating	Deterministic	Puertecitos, Mexico
[41]	–	–	–	Cost & emission	–	Power & heating & cooling	Stochastic	South China Sea Island
[24]	Fuzzy	Demand	–	Supply & demand Balance	–	Power & desalination	Deterministic	Liuheng Island, China
[8]	–	–	–	Cost	–	Power & heating & cooling	Stochastic	Kish Island, Iran
[42]	RA-IGDT	Demand & PV & WT & Price	–	Cost & emission	–	Power & heating & cooling	Stochastic	–
[43]	Robust	Demand & PV & WT	–	Cost & emission	–	Power & heating & cooling	Deterministic	–
[5]	Stochastic (CVaR)	Demand & PV & EVs	✓	Cost & emission	–	Power & heating & cooling	Stochastic	–
[7]	KL-based DRO	Demand & PV & WT & Price	✓	Cost & emission	–	Power & heating & cooling	Stochastic	–
[34]	–	–	–	Cost	–	Power & heating	Deterministic	–
[9]	Stochastic	Demand & PV & WT & Price	–	Cost & emission	–	Power & heating	Stochastic	–
[26]	Stochastic (LHS)	Demand & PV & WT	–	Cost & emission	–	Power & heating & cooling	Stochastic	–
[39]	–	–	✓	Cost	–	Power & desalination	Deterministic	Bruny Island, Australia
Current paper	RA-IGDT & RS-IGDT & Robust & CVaR	Demand & PV & WT & EVs	✓	Cost & emission	✓	Power & heating & cooling	Stochastic	Ontario, Canada

3. Investigating the impact of increasing the number of EVs on the total cost of the EH in both coordinated and uncoordinated charging modes, including participation in the V2G program.
4. Considering all EVs in the province of Ontario within the EH model and comparing the total costs of the EH with and without applying battery depreciation costs.
5. Using the CVaR method to deal with the uncertainty related to charging and discharging of EVs.

3. Energy hub structure

An energy hub is a comprehensive system that facilitates the integration and communication between multiple energy inputs and outputs. This system acts as a centralized management structure, optimizing energy flow, and ensuring efficient utilization of resources. The energy hub consists of three core elements: energy transmission devices, energy conversion devices, and energy storage devices.

Energy transmission devices transfer produced energy directly to the consumption side without conversion. Examples include electrical cables for electricity, and thermal pipelines for heating or cooling networks. Transmission efficiency is vital for minimizing losses during energy delivery.

Energy conversion devices enable the transformation of one form of energy into another, ensuring the flexibility and adaptability of the hub. Examples include gas turbines to generate electricity from natural gas, electric chillers, and absorption chillers to produce cooling energy using electricity and heat. These devices ensure the coupling between multiple energy carriers, enabling the hub to adapt to different operational scenarios.

Energy storage devices provide the capacity to store energy (electric, thermal, or cooling) to mitigate peak loads and reduce operational costs. Examples include batteries for electrical energy storage, thermal storage tanks for heat storage, and ice storage conditioners for cooling energy storage. Energy storage plays a crucial role in responding to demand and increasing resilience against uncertainty in energy supply.

An energy hub is a system that establishes communication between several energy inputs and outputs. An energy hub consists of various equipment, including energy transmission, energy conversion, and energy storage devices. Energy transmission devices directly transfer the produced energy to the consumption side without converting it. This category can include cables and thermal network pipelines, among others. Energy conversion devices are responsible for the conversion and coupling of all types of energy. This category can contain gas turbines, electric and absorption chillers, among others. Energy storage devices store electric, heating, or cooling energy to help reduce peak loads and related costs. Batteries, heat storage tanks, and ice storage conditioners fall under this category. The inputs and outputs of the energy hub, as well as their connection through the coupling matrix, follow a specific relationship, as illustrated in Fig. 1. This figure defines the correlation between input carriers and outputs within a multi-energy system, often represented as a coupling matrix:

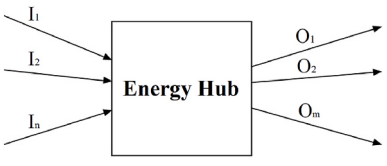

Fig. 1. An energy hub's input-output model.

$$\begin{bmatrix} O_1 \\ O_2 \\ \vdots \\ O_m \end{bmatrix} = \begin{bmatrix} C_{11} & C_{12} & \dots & C_{1n} \\ C_{21} & C_{22} & \dots & C_{2n} \\ \vdots & \vdots & \ddots & \vdots \\ C_{m1} & C_{m2} & \dots & C_{mn} \end{bmatrix} \begin{bmatrix} I_1 \\ I_2 \\ \vdots \\ I_n \end{bmatrix} \quad (1)$$

Where O is a $m \times 1$ matrix that expresses the outputs of the energy hub. C is a $m \times n$ matrix called the coupling matrix. Each element of C denotes the energy efficiency. I is a $n \times 1$ matrix that corresponds to the energy hub inputs.

The proposed energy management system encompasses power, cooling, and heating hubs. Energy hubs are examined in three primary domains: the production, consumption, and storage of electrical energy. In the realm of electrical energy generation, several primary sources come into play, including photovoltaic (PV) systems, wind turbines (WT), and the conventional power grid. The thermal energy production sector involves natural gas procured from the network. In addition, the cooling energy production sector encompasses both electricity purchased from the electrical network and natural gas acquired from the network. Within the consumption sector, there are three main areas of demand: electrical, heating, and cooling requirements. Furthermore, the storage section includes both heat and cold storage, as well as electric car parking.

Fig. 2 details the structure of the proposed energy hub. The studied hub consists of several main parts. The demand for electric energy can be directly supplied from PV, WT, hydro, nuclear, biofuel, and natural gas power plants. An indirect way to meet the electrical energy demand is to feed natural gas to the CCHP unit and generate electrical energy from the gas turbine. There are two ways to produce thermal energy: 1) using the heat output of the gas turbine unit; and 2) feeding natural gas into the gas boiler and producing heat. Due to the existence of V2G capability for electric vehicles, EV parking can also be considered as storage location for electrical energy. Thermal storage is also used for thermal energy storage applications. Heat or electricity can produce cooling energy. An electric chiller can use electricity to produce cooling energy. An absorption chiller can also receive electricity and heat at the same time, producing cooling energy. The ice storage conditioner uses electricity to store cooling energy.

The proposed energy hub provides several key advantages as follows.

1. Integration of renewable energy: by efficiently integrating PV and wind turbines, the energy hub maximizes the use of clean energy sources while balancing their intermittent nature through storage and flexible conversion.

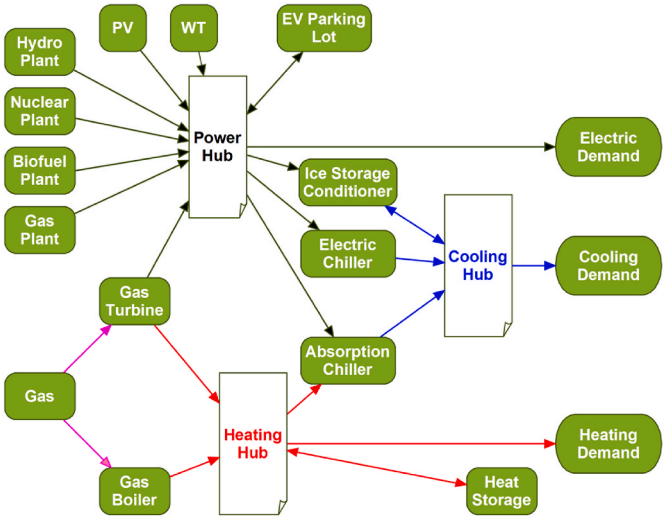

Fig. 2. Energy hub structure.

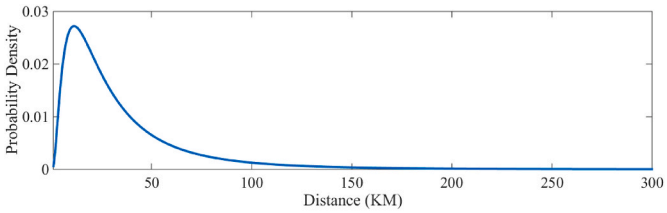

Fig. 3. Probability distribution function of the daily travel distance of the EVs.

2. Demand response and cost reduction: by incorporating time-of-use electricity pricing and storage devices, the energy hub reduces peak loads, leading to significant cost savings and better grid stability.
3. Flexibility and adaptability: the hub's design accommodates various energy sources and consumption patterns, making it suitable for varying operational scenarios and future expansions.
4. Emission reduction: efficient coupling and conversion processes reduce reliance on fossil fuels, contributing to lowering the greenhouse gas emissions.
5. Real-world application: the results of the energy hub model provide actionable insights for policymakers and energy operators, enabling informed decisions regarding infrastructure development, renewable energy integration, and demand-side management.

4. Optimization model

This section explains the mathematical modeling of the energy hub. The notation used for the model parameters and the main and auxiliary binary variables is introduced in the nomenclature.

4.1. The EV charging model

The lognormal distribution function can represent the daily travel distance of EVs in the energy hub structure optimization model and EV charging model. The lognormal distribution is commonly used to model positive-valued variables that exhibit skewed behavior [25]. In the context of EVs, this distribution captures the variability in daily driving distances, accounting for factors such as charging patterns, road conditions, and individual driving habits. This function defines the probability density associated with the EVs' travel distances as follows:

Fig. 3 illustrates the probability distribution associated with the daily travel distance of EVs. Additionally, Fig. 4considers the arrival and departure times of these EVs. Understanding the distribution of daily travel distances is crucial to optimizing EV charging infrastructure, predicting energy demand, and planning efficient routes. By analyzing the lognormal distribution of EV travel distances, researchers and policymakers can make informed decisions to promote sustainable transportation and reduce emissions.

The distance EVs travel during the day and the starting point of their charging are mutually independent. Specifications related to the process of charging each EV can be achieved with the help of random experi-

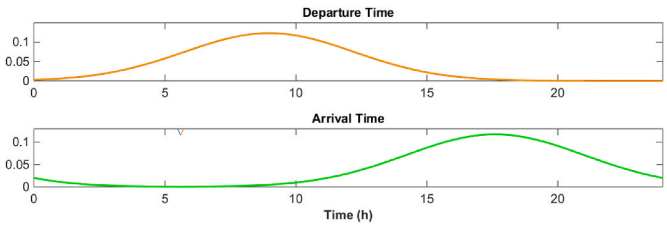

Fig. 4. Probability distribution functions of departure and arrival time of EVs.

ments so that the driving distance and the starting point of charging each EV can be simulated. Most of the studies that model EV entrance, distance traveled inside the energy hub, and exit, have used the Monte Carlo simulation method for their analysis. Accordingly, this paper uses the Monte Carlo simulation method as well. A lognormal distribution function with parameters $\sigma_s = 0.88$ and $\mu_s = 3.2$ can be used to model the daily driving distance of EVs [25]. The following describes the probability density function.

When EV owners leave their homes in the morning, they typically stop charging. An electric vehicle's departure time follows a normal distribution with $\sigma_{dep} = 8.92$ and $\mu_{dep} = 3.2$ [25]. When EV owners arrive home in the evening, they typically begin charging their vehicles. An EV's arrival time can be represented by a normal distribution with $\sigma_{arr} = 17.6$ and $\mu_{arr} = 3.4$.

$$f_s(x) = \frac{1}{\sqrt{2\pi}.\sigma_s.x} exp\left(-\frac{(\ln x - \mu_s)^2}{2\sigma_s^2} \right) \tag{2}$$

$$f_{dep}(t) = \begin{cases} \frac{1}{\sqrt{2\pi}.\sigma_{dep}} exp\left(-\frac{\left(t - \mu_{dep}\right)^2}{2\sigma_{dep}^2} \right) & 0 < t \le \mu_{dep} + 12 \\ \frac{1}{\sqrt{2\pi}.\sigma_{dep}} exp\left(-\frac{\left(t - 24 - \mu_{dep}\right)^2}{2\sigma_{dep}^2} \right) & \mu_{dep} + 12 < t \le 24 \end{cases} \tag{3}$$

$$f_{arr}(t) = \begin{cases} \frac{1}{\sqrt{2\pi}.\sigma_{arr}} exp\left(-\frac{(t + 24 - \mu_{arr})^2}{2\sigma_{arr}^2} \right) & 0 < t \le \mu_{arr} - 12 \\ \frac{1}{\sqrt{2\pi}.\sigma_{arr}} exp\left(-\frac{(t - \mu_{arr})^2}{2\sigma_{arr}^2} \right) & \mu_{arr} - 12 < t \le 24 \end{cases} \tag{4}$$

After this step, the total load profile can be calculated according to the load profile of each EV. The simulation operation will be performed N times for a certain number of EVs (M). The higher the number of M and N, the longer the simulation time, and the smoother the curve results. The specific steps to calculate the unbalanced charging load of electric vehicles are as follows (see Fig. 5).

Step 1: Start with the first iteration, $i = 1$.
Step 2: Start with the first EV, $j = 1$.
Step 3: Consider the probability density function of the arrival time and generate a random number of charging start times for the j - th EV.
Step 4: Consider the probability density function of the daily driving distance and generate a random quantity of travel distances for the j - th EV.
Step 5: Compute the power demand for charging and the charging duration of the j - th EV.
Step 6: Overlay the charging load profile of the j - th EV.
Step 7: If $j < M$, increment the EV index j by 1 and loop back to Step 3. Otherwise, go to the next step.
Step 8: If $i < N$, increment the iteration index i by 1 and loop back to Step 2. Otherwise, report the result, and the process concludes.

4.2. Objective function

The primary objective function aims to minimize overall costs, including transmission costs between energy hubs and the grid, energy conversion costs, carbon emission costs, battery depreciation costs, and the expenses associated with Demand Response (DR) programs. Thus, the main objective function is defined as follows:

$$OF = Cost_{OM} + Cost_{EM} + Cost_{Bat} + Cost_{DR} \tag{5}$$

Where $Cost_{OM}$ represents the total operational and maintenance costs, $Cost_{EM}$ denotes the total emission costs, $Cost_{Bat}$ stands for the total costs of EV batteries, and $Cost_{DR}$ represents the costs for demand response programs. In the following, each part is defined in detail:

$$Cost_{OM} = Cost_{OM}^{PP} + Cost_{OM}^{GT} + Cost_{OM}^{GB} + Cost_{OM}^{EC} + Cost_{OM}^{AC} + Cost_{OM}^{ISC} + Cost_{OM}^{HS} \tag{6}$$

$Cost_{OM}^{PP}$ is the total cost related to the operation and maintenance of power plant units, $Cost_{OM}^{GT}$ and $Cost_{OM}^{GB}$ are the operating and maintenance costs of gas turbine and gas boiler, respectively. $Cost_{OM}^{EC}$ and $Cost_{OM}^{AC}$ are the operating and maintenance costs of electric chiller and absorption chiller, respectively. $Cost_{OM}^{ISC}$ and $Cost_{OM}^{HS}$ are the operating and maintenance costs of the ice storage conditioner and heating storage unit, respectively. These are defined as follows:

$$Cost_{OM}^{PP} = Pr_t^e . \sum_t \left(P_t^{Nuc}.OM_{Nuc} + P_t^{Hyd}.OM_{Hyd} + P_t^{Bio}.OM_{Bio} + P_t^{Gas}.OM_{Gas} + P_t^{PV}.OM_{PV} + P_t^{WT}.OM_{WT} \right).\Delta t \tag{7}$$

Where Pr_t^e is a coefficient applied to the cost of buying electricity from the grid at different times of the day, according to peak and off-peak hours. OM_{Nuc}, OM_{Hyd}, OM_{Bio}, OM_{Gas}, OM_{PV}, OM_{WT} are the operating and maintenance costs per kilowatt-hour of electricity produced in nuclear, hydroelectric, biofuel, natural gas, solar, and wind power plants, respectively. Other operating and maintenance costs are defined in the following equations:

$$Cost_{OM}^{GT} = \sum_t \left(G_t^{GT}.\lambda_t^G + \left(P_t^{GT} + H_t^{GT} \right).OM_{GT}.\Delta t \right) \tag{8}$$

$$Cost_{OM}^{GB} = \sum_t \left(G_t^{GB}.\lambda_t^G + H_t^{GB}.OM_{GB}.\Delta t \right) \tag{9}$$

$$Cost_{OM}^{EC} = \sum_t P_t^{EC}.OM_{EC}.\Delta t \tag{10}$$

$$Cost_{OM}^{AC} = \sum_t H_t^{AC}.OM_{AC}.\Delta t \tag{11}$$

$$Cost_{OM}^{ISC} = \sum_t P_t^{ISC}.OM_{ISC}.\Delta t \tag{12}$$

$$Cost_{OM}^{HS} = \sum_t \left(H_{dch,t}^{HS} + H_{ch,t}^{HS} \right).OM_{HS}.\Delta t \tag{13}$$

The second term of the objective function equation (5) belongs to pollution emission costs. Power plants, gas turbines and gas boilers pollute the environment which should be considered in the energy hub costs.

$$Cost_{EM} = Cost_{EM}^{PP} + Cost_{EM}^{GT} + Cost_{EM}^{GB} \tag{14}$$

The terms included in equation (14) are defined as follows:

$$Cost_{EM}^{PP} = P_e^t . \sum_t \left(P_t^{Nuc}.EM_{Nuc} + P_t^{Hyd}.EM_{Hyd} + P_t^{Bio}.EM_{Bio} + P_t^{Gas}.EM_{Gas} + P_t^{PV}.EM_{PV} + P_t^{WT}.EM_{WT} \right).\Delta t \tag{15}$$

$$Cost_{EM}^{GT} = \sum_t \left(P_t^{GT} + H_t^{GT} \right).EM_{GT}.\Delta t \tag{16}$$

$$Cost_{EM}^{GB} = \sum_t H_t^{GB}.EM_{GB}.\Delta t \tag{17}$$

The third term of the objective function equation (5) is related to the depreciation costs of electric vehicle batteries, which is defined as follows:

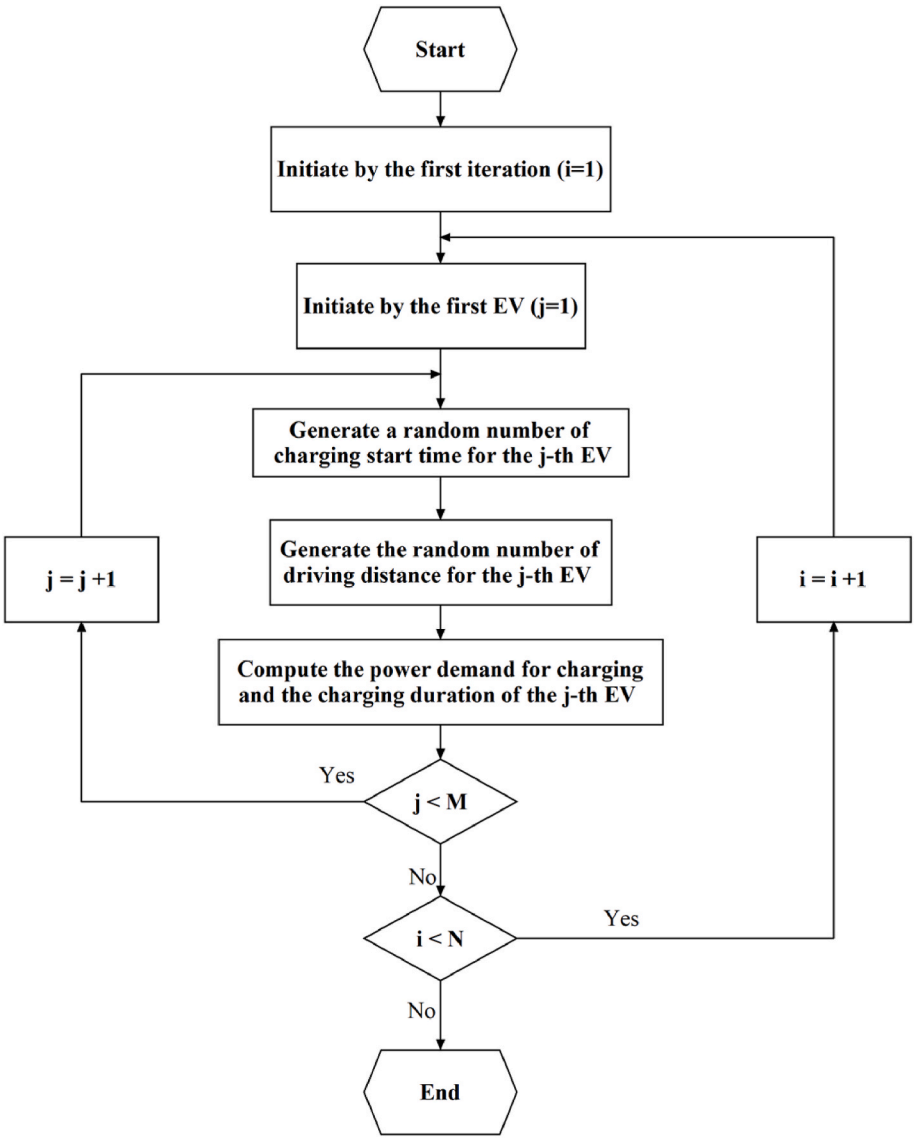

Fig. 5. Flowchart to calculate power demand for charging EVs.

$$Cost_{Bat} = \sum_t \sum_j \left(P^{EV}_{ch,j,t} + P^{EV}_{dch,j,t}\right).\frac{Rep^{EV}_j}{Cap^{EV}_j}.\Delta t \tag{18}$$

The last term of the objective function equation (5) belongs to the costs of applying demand response programs, which is defined as follows:

$$Cost_{DR} = \left(P^{up}_t.DR^E_{up} + P^{down}_t.DR^E_{down} + H^{up}_t.DR^H_{up} + H^{down}_t.DR^H_{down} + C^{up}_t.DR^C_{up} + C^{down}_t.DR^C_{down}\right).\Delta t \tag{19}$$

4.3. Operational constraints

4.3.1. Electric DR system constraints

The electric DR system constraints are defined as follows:

$$\sum_t P^{up}_t = \sum_t P^{down}_t \tag{20}$$

$$0 \le P^{up}_t \le MR^E_{up}.P^L_t.I^{E.up}_t \tag{21}$$

$$0 \le P^{down}_t \le MR^E_{down}.P^L_t.I^{E.down}_t \tag{22}$$

$$0 \le I^{E.up}_t + I^{E.down}_t \le 1 \tag{23}$$

4.3.2. Thermal DR program constraints

The thermal DR constraints are expressed as:

$$\sum_t H^{up}_t = \sum_t H^{down}_t \tag{24}$$

$$0 \le H^{up}_t \le MR^H_{up}.H^L_t.I^{H.up}_t \tag{25}$$

$$0 \le H^{down}_t \le MR^H_{down}.H^L_t.I^{H.down}_t \tag{26}$$

$$0 \le I^{H.up}_t + I^{H.down}_t \le 1 \tag{27}$$

4.3.3. Cooling DR program constraints

The cooling DR constraints are expressed as:

$$\sum_t C^{up}_t = \sum_t C^{down}_t \tag{28}$$

$$0 \le C_t^{up} \le MR_{up}^{C}.C_t^{L}.I_t^{C.up} \tag{29}$$

$$0 \le C_t^{down} \le MR_{down}^{C}.C_t^{L}.I_t^{C.down} \tag{30}$$

$$0 \le I_t^{C.up} + I_t^{C.down} \le 1 \tag{31}$$

4.3.4. EV constraints

The EV constraints are given by:

$$E_{j,t}^{EV} = E_{j,t-1}^{EV} + P_{ch,j,t}^{EV}.\Delta t.\eta_{ch}^{EV} - \frac{P_{dch,j,t}^{EV}.\Delta t}{\eta_{dch}^{EV}} \tag{32}$$

$$E_{min,j}^{EV} \le E_{j,t}^{EV} \le E_{max,j}^{EV} \tag{33}$$

$$0 \le P_{ch,j,t}^{EV} \le P_{ch,max,j}^{EV}.Z_{j,t}^{ch} \tag{34}$$

$$0 \le P_{dch,j,t}^{EV} \le P_{dch,max,j}^{EV}.Z_{j,t}^{dch} \tag{35}$$

$$Z_{j,t}^{ch} + Z_{j,t}^{dch} = 1, \forall j, t \in \left[t_{arr,j}, t_{dep,j}\right] \tag{36}$$

$$Z_{j,t}^{ch} + Z_{j,t}^{dch} = 0, \forall j, t \notin \left[t_{arr,j}, t_{dep,j}\right] \tag{37}$$

$$0 \le \sum_t P_{ch,j,t}^{EV} \le P_{ch,max}^{EV} \tag{38}$$

$$0 \le \sum_t P_{dch,j,t}^{EV} \le P_{dch,max}^{EV} \tag{39}$$

4.3.5. Thermal storage unit constraints

The constraints for the thermal storage unit are defined as:

$$E_t^{HS} = E_{t-1}^{HS} + H_{ch,t}^{HS}.\Delta t.\eta_{ch}^{HS} - \frac{H_{dch,t}^{HS}.\Delta t}{\eta_{dch}^{HS}} \tag{40}$$

$$E_{min}^{HS} \le E_t^{HS} \le E_{max}^{HS} \tag{41}$$

$$0 \le H_{ch,t}^{HS} \le H_{ch,max}^{HS}.K_t^{ch} \tag{42}$$

$$0 \le H_{dch,t}^{HS} \le H_{dch,max}^{HS}.K_t^{dch} \tag{43}$$

$$K_t^{ch} + K_t^{dch} \le 1 \tag{44}$$

4.3.6. Ice storage conditioner unit constraints

The constraints for ice storage conditioner unit are defined as:

$$E_t^{ISC} = E_{t-1}^{ISC} + P_t^{ISC}.\Delta t.\eta_{ch}^{ISC} - \frac{C_t^{ISC}.\Delta t}{\eta_{dch}^{ISC}} \tag{45}$$

$$E_{min}^{ISC} \le E_t^{ISC} \le E_{max}^{ISC} \tag{46}$$

$$0 \le P_t^{ISC} \le P_{t,max}^{ISC}.N_t^{ch} \tag{47}$$

$$0 \le C_t^{ISC} \le C_{t,max}^{ISC}.N_t^{dch} \tag{48}$$

$$N_t^{ch} + N_t^{dch} \le 1 \tag{49}$$

4.3.7. The natural gas constraints

The natural gas constraints are defined as:

$$0 \le G_t^{GT} \le G_{max}^{GT} \tag{50}$$

$$0 \le G_t^{GB} \le G_{max}^{GB} \tag{51}$$

$$0 \le H_t^{GT} + H_t^{GB} + H_{dch,t}^{HS} - H_{ch,t}^{HS} \le H_{max} \tag{52}$$

$$0 \le P_t^{PP} \le P_{TR}^{max} \tag{53}$$

$$0 \le P_t^{sell} \le P_{TR}^{max} \tag{54}$$

4.4. Energy balance in the energy hub system

The energy balance equations for thermal and electric energy in the EH system are arranged as follows:

$$P_t^{PP} + P_t^{GT} + \sum_j P_{dch,j,t}^{EV} + P_t^{E.down} = P_t^{L} + \sum_j P_{ch,j,t}^{EV} + P_t^{sell} + P_t^{E.up} + P_t^{EC} + P_t^{ISC} \tag{55}$$

$$P_t^{PP} = P_t^{PV} + P_t^{WT} + P_t^{Nuclear} + P_t^{Hydro} + P_t^{Biofuel} + P_t^{Gas} \tag{56}$$

$$H_t^{GT} + H_t^{GB} + H_{dch,t}^{HS} + H_t^{down} = H_t^{L} + H_{ch,t}^{HS} + H_t^{up} + H_t^{AC} \tag{57}$$

$$C_t^{EC} + C_t^{AC} + C_t^{ISC} = C_t^{L} \tag{58}$$

$$H_t^{GB} = G_t^{GB}.V_{Gas}.\eta_{GB}/\Delta t \tag{59}$$

$$P_t^{GT} = G_t^{GT}.V_{Gas}.\eta_{GT}^{e}/\Delta t \tag{60}$$

$$H_t^{GT} = G_t^{GT}.V_{Gas}.\eta_{GT}^{h}/\Delta t \tag{61}$$

$$P_t^{EC}.COP_{EC} = C_t^{EC} \tag{62}$$

$$H_t^{AC}.COP_{AC} = C_t^{AC} \tag{63}$$

$$P_t^{ISC}.COP_{ISC} = C_t^{ISC} \tag{64}$$

4.5. Modeling uncertainty

The described energy hub system has several uncertain elements. For example, the amount of power produced by renewable sources, especially wind turbines, is quite uncertain and very difficult to predict. In some cases, the water reservoir of a dam can decrease to such an extent that hydroelectric plants also face the problem of uncertainty. Furthermore, the price of natural gas changes on a daily basis, leading to variations in the cost of producing electricity.

In contrast, nuclear, natural gas, and biofuel power plants rarely experience uncertainty. For example, although a high-capacity nuclear power plant may become unoperational, in general, the amount of power produced by the named power plants is very stable and does not include uncertainties. Additionally, gas turbines and gas boilers, which are also considered generators in a CCHP system, are not considered sources of uncertainty.

The demand side of the energy hub contains many uncertainties. For example, the demand for electrical, thermal, and cooling energy may show significant variations from the predicted amount. The other sources of uncertainty of demand include the charging and discharging times of electric vehicles as well as the amount of energy needed to charge each car every day. Therefore, the demand for energy is one of the most important sources of uncertainty.

To deal with uncertainty in energy hubs, various methods have been proposed, including stochastic optimization, robust modeling, and IGDT methods. The advantage of the stochastic method is its relative ease of modeling. However, it requires defining several scenarios to reach an acceptable result, which is time-consuming. In recent years, many studies have employed the CVaR method to model uncertainty. The main objective of the CVaR method is to reduce the risk of the worst-case scenario happening. The robust method defines the worst-case scenario and aims to improve this worst-case as much as possible. The IGDT method has two distinct approaches: risk seeker and risk averse. This method determines a specific amount of profit or loss and defines an

acceptable range for uncertain parameters. As mentioned before, this paper employs robust optimization, RA-IGDT, and RS-IGDT approaches to deal with uncertainty. This paper employs the CVaR method to address the uncertainties associated with the charging profile of electric vehicles. This section presents these four methods in detail along with their corresponding equations.

Uncertainty analysis was performed using the RA-IGDT, RS-IGDT, and Robust Optimization methods. These approaches quantify the impacts of uncertainties in key parameters by defining allowable deviations and assessing their effects on the total energy hub cost. The results provide insight into the system's robustness and performance under varying levels of uncertainty, ensuring reliable decision-making.

In addition to RA-IGDT, RS-IGDT, and Robust Optimization methods, the CVaR (Conditional Value at Risk) method is employed to address uncertainties specifically related to EV behaviors, such as travel distances and charging patterns. While the primary focus of this study is on the three core methods, CVaR improves the framework by ensuring robustness in decisions related to EV operations in worst-case scenarios.

4.5.1. The robust approach

In an energy hub, volatility of electricity prices presents challenges for efficient energy distribution. Consequently, identifying an appropriate strategy to address price uncertainty becomes crucial. Traditional stochastic programming relies on generating numerous scenarios using the probability distribution function of electricity prices. Nevertheless, the process of fitting a distribution using the actual prices and realizing the distribution function is intricate and time consuming. In contrast, robust optimization, as a viable alternative, does not require any knowledge of the probability distribution function for uncertain data. Instead, it characterizes the range of uncertain parameters by utilizing an uncertainty set, which may be readily created using current forecasting approaches. Therefore, in this section, a robust optimization approach is implemented to tackle the uncertainty associated with electricity prices.

This paper constructs uncertainty sets to address the unpredictability of electricity prices (65), the amount of power produced using renewable sources including photovoltaic (66) and wind energy (67), the demand for electricity (68), and the thermal and cooling demand (69) and (70), respectively. These uncertainty sets are outlined below:

$$Pr_t^e \in \left[\widehat{Pr}_t^e, \widehat{Pr}_t^e + \beta_t^1 . d_t^1\right] \tag{65}$$

$$P_t^{PV} \in \left[\widehat{P}_t^{PV} - \beta_t^2 . d_t^2, \widehat{P}_t^{PV}\right] \tag{66}$$

$$P_t^{WT} \in \left[\widehat{P}_t^{WT} - \beta_t^3 . d_t^3, \widehat{P}_t^{WT}\right] \tag{67}$$

$$P_t^L \in \left[\widehat{P}_t^L, \widehat{P}_t^L + \beta_t^4 . d_t^4\right] \tag{68}$$

$$H_t^L \in \left[\widehat{H}_t^L, \widehat{H}_t^L + \beta_t^5 . d_t^5\right] \tag{69}$$

$$C_t^L \in \left[\widehat{C}_t^L, \widehat{C}_t^L + \beta_t^6 . d_t^6\right] \tag{70}$$

$$0 \le \beta_t^i \le 1 \tag{71}$$

$$\sum_t \beta_t^i \le \Gamma \tag{72}$$

$$i = 1, 2, \ldots, 6$$

In robust optimization, d_t^i parameters play a crucial role in modeling uncertainties, where each parameter is defined as an uncertain variable that may deviate from its nominal value. d_t^1, d_t^2, d_t^3, d_t^4, d_t^5, and d_t^6 parameters represent the potential deviation of the energy price, PV output power, wind turbine output power, electrical load, heating load, and cooling load from their nominal values, respectively. Hence, the changes in the variables include P_t^{PV}, P_t^{WT}, and Pr_t^e in Equation (7), P_t^{PV} and P_t^{WT} in Equation (15), P_t^L in Equation (55), P_t^{PV} and P_t^{WT} in Equation (56), and H_t^L and C_t^L in Equations (57) and (58), respectively. The main objective function of the problem is to minimize the overall costs of the energy hub, as defined in Equation (5). For more information on dealing with uncertainty using robust optimization, the reader is referred to Ref. [28].

4.5.2. The IGDT method

Various parameters contribute to uncertainty in this optimization problem, each of which can affect the performance of the system, positively or negatively. In this article, the Information Gap Decision Theory (IGDT) method is used to account for the different uncertainties present in the system. The following provides a brief description of the IGDT method [44]. The optimization problems can be expressed as follows.

$$f = \min\left(f(X, \lambda)\right) \tag{73}$$

$$H(X, \lambda) \le 0 \tag{74}$$

$$G(X, \lambda) = 0 \tag{75}$$

$$\lambda = U \tag{76}$$

where λ represents the uncertainty parameter, U is the set of uncertainties affecting the behavior of uncertain input parameters, and X represents the set containing the decision variables of the problem. Mathematically, uncertainty can be described using a fractional error model within the IGDT method as follows:

$$U(\alpha, \lambda_1) = \left\{\lambda_t : \frac{|\lambda_t - \lambda_1|}{\lambda_t} \le \alpha\right\}, \alpha \ge 0 \tag{77}$$

where, α is known as the uncertainty radius (or uncertainty parameter). If the uncertain parameter deviates from its predicted value, the decision-maker faces either a risk-averse or risk-seeking strategy.

4.5.2.1. The risk-averse strategy (RA). This approach tackles scenarios where uncertainty in a parameter adversely affects the objective function. Consequently, the primary aim of this approach is to determine the largest uncertainty range for a given objective function value. This strategy optimizes the decision variables so that, given an increase in the objective function value, the maximum uncertainty range for the uncertain parameter remains within the acceptable bounds. In other words, this approach enhances the sturdiness of the objective function against errors in predicting input uncertainties. In simpler terms, the decision maker can have confidence that the objective function will not exceed a predefined threshold even when there are variations within the identified uncertainty range. This strategy is formally defined as follows [44].

$$\widehat{\alpha}(C_r) = \max \alpha \tag{78}$$

$$H(X, \lambda) \le 0 \tag{79}$$

$$G(X, \lambda) = 0 \tag{80}$$

$$f(X, \lambda) \le C_r \tag{81}$$

$$C_r = f_b(X, \lambda) \times (1 + \omega) \tag{82}$$

$$0 \le \omega \le 1 \tag{83}$$

where C_r represents the maximum allowable increase in the objective function, relative to the base value set by the decision maker. This base value is a function of the base value of the original objective function. The variable $\widehat{\alpha}(C_r) \ge 0$ denotes the uncertainty radius associated with

the problem's uncertain parameter. Additionally, ω signifies the increase in the objective function due to uncertainty, as determined by the decision maker. Within the proposed model, the maximum uncertainty radius $\widehat{\alpha}(C_r)$ is determined such that the objective function value remains within the allowable range, as specified in the relationship above.

To apply this method, the following steps were taken. In the first stage, the optimization problem was solved without considering uncertainties, and the objective function value was determined. In the second stage, the variable OF in Equation (5) is transformed into $C_r = OF \times (1+\omega)$. Each uncertainty parameter is assigned a weight factor. Thus, the uncertainty parameters in Equations ((7) and (15) and (55)–(58) are transformed into variables defined below.

$$P_t^{PV} = (1-\alpha_t^1)P_t^{PV} \tag{84}$$

$$P_t^{WT} = (1-\alpha_t^2)P_t^{WT} \tag{85}$$

$$Pr_t^e = (1+\alpha_t^3)Pr_t^e \tag{86}$$

$$P_t^L = (1+\alpha_t^4)P_t^L \tag{87}$$

$$H_t^L = (1+\alpha_t^5)H_t^L \tag{88}$$

$$C_t^L = (1+\alpha_t^6)C_t^L \tag{89}$$

Additionally, the objective function of the optimization problem is transformed into maximizing the deviation of the uncertainty parameters from the predicted value (i.e., max α).

4.5.2.2. The risk-seeker strategy (RS). Risk seeking refers to an individual's willingness to accept greater risk in exchange for the potential for higher returns. In the context of energy hubs, this often refers to fluctuations in electricity prices, energy demands, and the amount of renewable energy generation. Risk seeker operators prefer to consider the values of the uncertain parameters such that the total costs are lower than the predicted state, while accepting the risk of power outages during peak hours. Within the framework of IGDT, the risk seeking approach looks to maximize opportunities by embracing uncertainty. It involves making decisions that carry the potential for higher rewards, even if they entail an increased risk. When applying IGDT to decision making, the risk seeker strategy aims to exploit uncertainty rather than avoid it, with a focus on maximizing benefits while acknowledging the inherent risks. In summary, the risk seeker strategy within IGDT encourages a more adventurous approach, aiming for greater gains despite the associated uncertainties. This approach contrasts with the risk-averse strategy, which prioritizes minimizing losses and preserving capital. The equations are similar to the risk-averse case. Mathematically, this strategy is defined as follows [44].

$$\widehat{\alpha}(C_r) = \min \alpha \tag{90}$$

$$H(X,\lambda) \le 0 \tag{91}$$

$$G(X,\lambda) = 0 \tag{92}$$

$$f(X,\lambda) \le C_r \tag{93}$$

$$C_r = f_b(X,\lambda) \times (1-\omega) \tag{94}$$

$$0 \le \omega \le 1 \tag{95}$$

To apply this method, the first stage is the same as the risk-averse method and the same value obtained for OF is used. In the second stage, the variable OF in Equation (5) is transformed into $C_r = OF \times (1-\omega)$. Thus, the uncertainty parameters in Equations ((7) and (15) and (55)–(58) are transformed into the following variables.

$$P_t^{PV} = (1+\alpha_t^1)P_t^{PV} \tag{96}$$

$$P_t^{WT} = (1+\alpha_t^2)P_t^{WT} \tag{97}$$

$$Pr_t^e = (1-\alpha_t^3)Pr_t^e \tag{98}$$

$$P_t^L = (1-\alpha_t^4)P_t^L \tag{99}$$

$$H_t^L = (1-\alpha_t^5)H_t^L \tag{100}$$

$$C_t^L = (1-\alpha_t^6)C_t^L \tag{101}$$

Additionally, the objective function of the optimization problem is transformed into minimizing the deviation of the uncertainty parameters from the predicted value (i.e., min α).

4.5.3. The CVaR method

The Conditional Value at Risk (CVaR) approach serves as a powerful tool for decision making in uncertain contexts, with an application that extends to optimizing energy hubs. Unlike optimization methods that target the expected value, the CVaR approach prioritizes robustness by minimizing the risk associated with deviations from the anticipated outcome. A risk-averse approach involves quantifying the likelihood of unfavorable outcomes using a specific metric. Various risk measures can be employed for this purpose, with variance being a common choice. A high variance indicates a greater probability of deviating from the expected outcome. However, variance has limitations. For example, it penalizes positive deviations (such as high profits or low costs). In contemporary decision making, the widely adopted risk measure is Conditional Value-at-Risk (CVaR). In the context of cost distribution, CVaR can be roughly defined as the expected cost in worst-case scenarios. The popularity of the CVaR method among decision makers underscores its significance.

By considering $\alpha \in (0,1)$ and determining a *cost* distribution, CVaR is the expected value of a cost greater than the $(1–\alpha)$-quantile of the cost distribution [45]. By determining a *profit* distribution, CVaR is the expected value of a profit smaller than the $(1–\alpha)$-quantile of the profit distribution.

For mathematical formulation, the distance traveled denoted by equation (2) is considered as a probability density function, and the VaR and CVaR values should be calculated. The cumulative probability up to a distance x (VaR) should be equal to the confidence level α:

$$P(X \le VaR) = \alpha \tag{102}$$

In discrete form:

$$\sum_{i|x_i \le VaR} f_s(x_i).\Delta x = \alpha \tag{103}$$

The VaR at confidence level α is the distance x such that the cumulative probability equals α:

$$VaR = x_\alpha \tag{104}$$

CVaR is the expected value of X given that X is greater than VaR:

$$CVaR_\alpha = E[X|X \rangle VaR_\alpha] \tag{105}$$

In discrete form:

$$CVaR = \frac{\sum_{i|x_i \le VaR} x_i . f_s(x_i).\Delta x}{1-\alpha} \tag{106}$$

It is important to note that the CVaR method in this study is applied exclusively to the modeling of electric vehicles (EVs) to address uncertainties in their travel distances and charging behaviors. The method is not extended to the broader energy hub structure, which is analyzed using other optimization approaches.

By integrating the CVaR method with the lognormal distribution of

the EV travel distances, the model accounts for extreme scenarios in the energy demand from EVs. Equations (102)–(106) provide the mathematical framework for calculating the VaR and CVaR values, ensuring that the model remains robust under uncertainty. This focus on EVs allows for a targeted application of CVaR, allowing the system to effectively manage the risks associated with EV integration.

5. Simulation results

5.1. Case study

In this paper, the province of Ontario, Canada, is chosen as the case study due to its diverse energy mix, significant adoption of electric vehicles (EVs), and advanced energy policies. Ontario's energy system is supported by a variety of power generation sources, including nuclear, hydroelectricity, natural gas, wind, solar, and bioenergy. Table 2 provides the maximum capacity of these power plants, with data sourced from Ref. [46], a comprehensive report by the Canada Energy Regulator (CER). Nuclear power plants dominate the energy mix with a capacity of 12,633 MW, providing a stable base load, while hydroelectricity contributes 9648 MW, offering flexibility and peak demand support. Renewable energy sources, including wind and solar, collectively contribute 4200 MW but are subject to variability due to weather conditions.

Ontario also has a well-established infrastructure for energy distribution. According to CER [46], the province relies on interconnected pipelines, transmission lines, and storage facilities systems to ensure the stability and reliability of the energy supply. The presence of advanced infrastructure and a diverse energy mix makes Ontario an ideal location for evaluating the integration of EVs into the energy system.

The data used to model the energy hub in this study include maintenance costs per kilowatt-hour of electricity production, the efficiency levels of various units, and penalty factors for pollutant emissions. These values, along with additional parameters necessary for energy hub optimization, are summarized in Table 3. In this paper, three distinct scheduling scenarios are analyzed to investigate the impact of EV integration on Ontario's energy system.

1. Uncoordinated charging: in this scenario, EVs are charged without any coordination, leading to increased peak demand and increased dependence on natural gas power plants, which have a capacity of 7000 MW. This approach is less efficient and may result in higher operating costs and emissions.
2. Coordinated charging: this scenario optimizes EV charging schedules based on energy prices. By shifting charging to off-peak hours, this strategy minimizes the costs and enhances the utilization of nuclear and hydroelectric resources, reducing dependency on fossil fuel-based generation.
3. Vehicle-to-Grid (V2G): the third scenario leverages the V2G technology, enabling EVs to act as energy storage units. In this approach, EVs store surplus electricity during off-peak hours and inject energy back into the grid during peak demand periods. This scenario also integrates thermal and cooling storage units, as well as demand response programs, to further improve the efficiency and sustainability of the energy hub. The use of V2G allows for a better utilization of renewable energy sources, addressing their intermittent nature.

Table 2
Capacity of various types of power plants [47].

Type of power plant	Capacity (MW)
Nuclear	12,633
Hydroelectricity	9648
Natural gas	7000
Wind	3800
Solar	400
Bioenergy	300

Table 3
Required parameters for simulations [2,25,48], and [49].

Adopted Based on [48]		Adopted Based on [49]	
Parameter	Value	Parameter	Value
OM_{Nuc}	\$0.037/kWh	EM_{Nuc}	\$0.0022/kWh
OM_{Hyd}	\$0.032/kWh	EM_{Hyd}	0
OM_{Bio}	\$0.047/kWh	EM_{Bio}	\$0.0022/kWh
OM_{Gas}	\$0.045/kWh	EM_{Gas}	\$0.0063/kWh
OM_{PV}	\$0.0175/kWh	EM_{PV}	0
OM_{WT}	\$0.025/kWh	EM_{WT}	0
OM_{GT}	\$0.034/kWh	EM_{GT}	\$0.0058/kWh
OM_{GB}	\$0.039/kWh	EM_{GB}	\$0.0058/kWh
Adopted Based on [2]			
η^{HS}_{ch}	0.9	E^{ISC}_{min}	4000 MWh
η^{HS}_{dch}	0.9	E^{ISC}_{max}	20000 MWh
E^{HS}_{min}	5000 MWh	G^{GT}_{max}	2000 m^3/h
E^{HS}_{max}	20000 MWh	G^{GB}_{max}	2000 m^3/h
$H^{HS}_{ch,max}$	5000 MW	η_{GB}	0.8
$H^{HS}_{dch,max}$	5000 MW	η^{e}_{GT}	0.35
η^{ISC}_{ch}	0.9	η^{h}_{GT}	0.45
η^{ISC}_{dch}	0.88	COP_{EC}	4
$P^{ISC}_{t,max}$	4000 MW	COP_{AC}	1.2
$C^{ISC}_{t,max}$	4000 MW	COP_{ISC}	3.5
Adopted Based on [25]			
λ^{G}_{t}	\$0.022/m^3	DR^{C}_{down}	\$0.001/kWh
OM_{EC}	\$0.015/kWh	MR^{E}_{up}	0.5
OM_{AC}	\$0.005/kWh	MR^{E}_{down}	0.2
OM_{ISC}	\$0.010/kWh	MR^{H}_{up}	0.5
OM_{HS}	\$0.010/kWh	MR^{H}_{down}	0.2
Rep^{EV}_{j}	\$3000	MR^{C}_{up}	0.5
Cap^{EV}_{j}	60000 kWh	MR^{C}_{down}	0.2
DR^{E}_{up}	\$0.001/kWh	η^{EV}_{ch}	0.9
DR^{E}_{down}	\$0.001/kWh	η^{EV}_{dch}	0.9
DR^{H}_{up}	\$0.001/kWh	$P^{EV}_{ch,max,j}$	10 kW
DR^{H}_{down}	\$0.001/kWh	$P^{EV}_{dch,max,j}$	10 kW
DR^{C}_{up}	\$0.001/kWh		

To ensure the validity of the case study, the results of these scenarios are analyzed based on key performance indicators, including total energy costs, emissions, and grid reliability. The study provides insight into how EV integration, when combined with coordinated charging and advanced technologies such as V2G, can improve the operation of Ontario's energy system while reducing costs and emissions. The data used in this study are aligned with the provincial energy profiles published by CER [47], ensuring accuracy and relevance. Ontario's energy mix and advanced infrastructure present a unique opportunity to analyze the impact of EV integration and related technologies, making this case study a valuable contribution to understanding the future of sustainable energy systems.

In this paper, the data related to the existing power plants in the province of Ontario, Canada, is used for power generating plants. Table 2 shows the maximum capacity of various types of power plants in Ontario. All the data related to the maintenance costs per kilowatt-hour of electric energy production, the efficiency of all the units in the energy hub, the values of penalty factors considered for the emission of pollution, and other data needed for the energy hub modeling are given in Table 3.

In this paper, three scheduling scenarios are considered. In the first scenario, electric vehicles are charged in an uncoordinated manner. In the second scenario, electric vehicles are charged in a coordinated manner and according to the price of energy. In the third scenario, electric vehicles can participate in the V2G mode and store electrical

energy. Furthermore, in this scenario, thermal and cooling storage units as well as demand response programs are implemented.

There are several assumptions in this study.

1. Energy demand breakdown: The total daily energy demand for Ontario was used as the overall energy input to the model. However, no specific data source provides a detailed breakdown of this energy into electricity, heating, and cooling demands.

To address this, we utilized the proportional demand ratios provided in Ref. [2]. These ratios allowed us to estimate the distribution of total energy into the three categories, ensuring a reasonable approximation in the absence of direct measurements.

2 Parameters for optimization methods: The coefficients for the robust optimization method were adopted directly from a referenced study. For the IGDT methods (RS-IGDT and RA-IGDT), the parameters were adjusted to closely align with those used in the robust method. This approach allowed for a meaningful comparison between optimization methods under similar conditions.

3 EV behavioral modeling: The EV travel distances, arrival and departure times were modeled using predefined probability distributions (lognormal and normal) with parameters derived from credible references. These assumptions reflect realistic EV behaviors and were chosen to capture the variability in daily driving patterns and charging habits.

The following steps were taken to validate the proposed model.

1. Real-world data: The total energy demand data for Ontario were used as a reference for validation. This ensures that the model's input is grounded in real-world conditions observed in the province.
2. Comparative analysis: The robustness of the IGDT methods was validated by comparing their results with those obtained from the robust optimization approach. The similarity in the parameters ensured a fair and reliable comparison.
3. Monte Carlo simulations: Monte Carlo simulations were used to model the stochastic behaviors of EVs, adding robustness to the model by accounting for uncertainties in travel distances and charging patterns.
4. Scenario analysis: The model was tested under three different scenarios (uncoordinated charging, coordinated charging, and participation in V2G). These scenarios simulate real-world operational strategies and demonstrate the model's adaptability to varying conditions.

The simulation environment for this study includes the use of GAMS software, with CPLEX and BARON solvers employed to address the MIP optimization problem. These solvers were selected due to their strong ability to solve mixed-integer programming (MIP) problems efficiently. For uncertainty modeling related to electric vehicles (EVs), a sampling size of 500,000 was used. Although this larger sampling size increased the computational time, it significantly improves the accuracy and reliability of the results. The simulations were conducted on a PC equipped with an Intel Core i7 processor (2.6 GHz) and 16 GB of RAM, ensuring sufficient computational power to handle the complexity of the optimization tasks.

5.2. Numerical results

In both RS-IGDT and RA-IGDT methods, a 5 % coefficient was applied to model uncertainties in demand, electricity prices, and renewable energy production. This coefficient was chosen in line with the related literature, which evaluates IGDT coefficients ranging from 0 % to 25 % to balance robustness and optimization.

In the RS-IGDT method, the 5 % coefficient defines the bounds, within which the uncertainty parameters must deviate to achieve a 5 % reduction in the total EH costs. Similarly, in the RA-IGDT method, the same coefficient defines the maximum tolerable deviations that result in a 5 % increase in total EH costs. These values were derived iteratively using the mathematical frameworks of RS-IGDT and RA-IGDT.

The percentages for uncertain parameters (e.g., demands, electricity prices, wind power, and solar power) were derived from solving an optimization problem. In this problem, the total energy hub cost was treated as a parameter with a fixed value, while the uncertain parameters were modeled as decision variables subject to constraints derived from related studies. The constraints ensured that the deviations of uncertain parameters remained within realistic and operationally feasible ranges. The optimization problem aimed to maximize or minimize the uncertain parameters depending on the method (RS-IGDT or RA-IGDT) while maintaining the predefined cost thresholds.

In the RS-IGDT method, the minimum deviation from the predicted value for the uncertainty parameters (where the deviations result in a reduction in the total energy hub costs) achieved a 5 % reduction in the total energy hub costs compared to the predicted value. By assuming total costs as constant and solving the optimization problem using the RS-IGDT method to minimize the optimization variable, the following values are obtained. The results of this method indicate that if electrical, thermal and cooling demands, and electricity prices, decrease by at least 2.78 % and the energy produced by wind and solar power plants increases by at least 5.2 % and 1.4 %, respectively, this goal can be achieved, resulting in total energy hub costs that are 5 % lower than the predicted value. In contrast, in the RA-IGDT method where deviations result in increased costs, the maximum deviation from the predicted value for uncertainty parameters was calculated considering a 5 % higher cost than the predicted state. By assuming the total costs as constant and solving the optimization problem using the RA-IGDT method to maximize the optimization variable, the following values are obtained. The results indicate that if the electrical, thermal, and cooling demands as well as the electricity prices increase by a maximum of 4.8 %, and the energy produced by the wind and solar power plants decreases by a maximum of 8.4 % and 2.5 %, respectively, the total EH costs will be 5 % higher than the predicted value. In the robust method, the total costs of the EH were calculated taking into account the worst-case scenario for the uncertainty parameters. In this study, the coefficient d_t was set to 0.05 for demands and electricity costs, 0.1 for wind power generation, and 0.025 for solar power generation.

The parameter Γ is known as the robust parameter. Taking into account the 24-h daily schedule, it can have a value between 0 and 24. A value of 0 means that uncertainty is not considered, and a value of 24 means that the maximum uncertainty is applied. Selecting this value should be a trade-off between optimization and robustness. The robust parameter for the power generated by PV is maximized for values greater than 12 because there is no solar power generation for 12 h of the day. In this paper, to have a trade-off between optimization and robustness, Γ is considered 12. If Γ is chosen as 0, 12, and 24, the minimum total cost (objective function) in the first scenario will be 21,663, 23,486, and 25,021 in thousands of dollars, respectively.

Figure 1 in appendix shows the optimal power distribution for RA-IGDT, RS-IGDT, and robust methods under scenario 1, where electric vehicles are charged in a non-coordinated way. According to this figure, EVs charge when entering the parking lot and according to their profile, the most charging occurs during peak hours, causing the costs to increase. This figure demonstrates that the power produced during peak hours is the highest in the robust method (Tableau c). Afterward, RA-IGDT (Tableau a) produces the most power during the peak hours, while RS-IGDT (Tableau b) requires the least amount of power produced during the peak hours. Furthermore, the EV charging pattern is similar for all three methods, that is, more EVs are charged during peak hours when the price of electricity is higher. Figure 1-(d) shows the load diagram related to the uncoordinated charging of EVs for three different values of electric vehicles. As of October 2023, there were about

118,000 EVs registered in Ontario. Experts predict that Ontario will have 1,000,000 EVs by 2030 [46].

In Figure 2-(d) of Appendix, the price factor is defined for different hours of the day. This coefficient is defined according to off-peak hours, medium load hours, and peak-load hours to improve the response to demand in the energy hub system. Clear communication about the price factor with energy consumers will allow for better planning of electricity consumption during the day according to the price. Figure 2 in Appendix shows the optimal distribution of electrical power for all three methods in scenario 2, where electric vehicles are charged in a coordinated way. In this scenario, EVs are charged during off-peak times. In this scenario the amount of electric power produced during peak hours has decreased compared to scenario 1. Similarly to scenario 1, in this scenario, the robust method produces the most amount of electrical energy during peak hours (Tableau c). In the RS-IGDT method, the consumption amount is less than the predicted value. The load generated by PV and WT in the RS-IGDT method is slightly higher than the predicted value, while in the robust and RA-IGDT methods, the power generated by PV and WT is lower than the predicted value.

Figure 3 in Appendix shows the optimal distribution of electric power for all the three methods in scenario 3 (participation of EVs in V2G mode, using heat storage and ISC units, and applying DR programs). P_ISC is added in this scenario, which belongs to the power consumption of the ISC unit for cooling energy storage. As can be seen, the power related to electric vehicles has a negative value in some hours, which means that EVs have participated in V2G mode, i.e. they have been charged in non-peak hours and injected electricity into the network during peak hours. The implementation of demand response programs has caused the curve related to electric load demand to change and the maximum electric energy demand to decrease.

Figure 4, 5 and 6 in Appendix show the thermal energy distribution of all the three methods for scenarios 1, 2, and 3, respectively. As can be seen, the maximum amount of thermal energy demand for the robust method is higher than the RA-IGDT method. In addition, the maximum amount of thermal energy demand in RS-IGDT method is about 3 % less than the predicted value. The thermal energy distribution in scenarios 1 and 2 are similar, but in scenario 3, it has changed with the addition of thermal energy storage. Also, the thermal energy demand has changed and improved due to the implementation of demand response programs.

Figure 7, 8 and 9, in the Appendix show the cooling energy distribution of all three methods for scenarios 1, 2, and 3, respectively. As can be seen, the maximum amount of cooling energy demand for the RS-IGDT method is lower than those of the others and it is the highest in the robust method. The distribution of cooling energy also changes in scenario 3 with the addition of the ISC unit. When the ISC unit is added to the figures, it consumes electric charge during non-peak hours and converts it into cooling energy. However, during peak hours, the ISC unit injects energy into the network. The demand for cooling energy has also changed due to the implementation of demand response programs, where its peak value has decreased.

Table 4 presents the total cost for the three mentioned methods when applying various scenarios with and without considering the depreciation cost of EVs using equation (18). Naturally, not considering the depreciation cost of EVs results in the reduction of the total cost. In other words, the model charges and discharges the EVs more frequently in the V2G program (scenario 3). Subsequently, applying the depreciation cost of batteries leads to more regulated V2G results (see Fig. 6). Additionally, a baseline scenario has been added for comparison, representing the case in which none of the uncertainty management methods are applied. This baseline provides a reference to evaluate the effectiveness of the proposed strategies in reducing costs and effectively managing uncertainties.

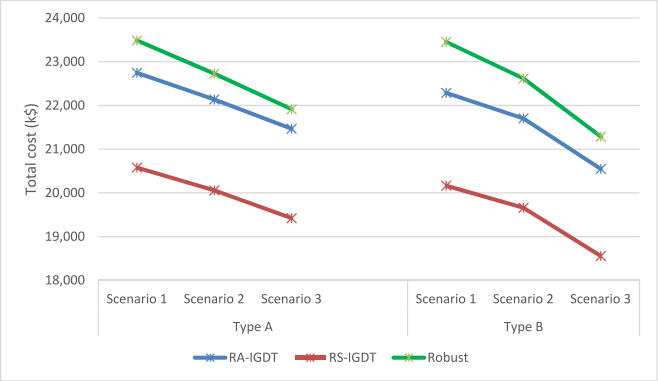

Fig. 6. Total costs for all methods under different scenarios.

Table 5
Improvement percentages of total cost when changing scenarios.

Approach	Improvement percentage of total cost			
	Type A		Type B	
	From scenario 1 to scenario 2	From scenario 2 to scenario 3	From scenario 1 to scenario 2	From scenario 2 to scenario 3
RA-IGDT	2.68	3.02	2.63	5.32
RS-IGDT	2.54	3.16	2.51	5.61
Robust	3.23	3.58	3.56	5.88
Baseline	2.37	2.71	2.45	5.18

Table 5 presents the percentages of improvement of the total cost when transitioning between scenarios for the three methods (RA-IGDT, RS-IGDT, and Robust) applied to two types of systems (Type A and Type B). These percentages represent the cost reductions achieved through the implementation of coordinated charging (scenario 2) and the V2G program (scenario 3).

For both types of systems, the transition from scenario 1 to scenario 2 results in noticeable cost reductions due to a better alignment of EV charging with electricity price variations. Further cost improvements are observed when moving from scenario 2 to scenario 3, highlighting the effectiveness of the V2G program in utilizing EVs as energy storage systems. Additionally, a baseline scenario has been included for comparison. The baseline represents a case where no uncertainty management methods are applied, providing a reference point to evaluate the relative improvements achieved by each method. The results show that while the baseline scenario also achieves cost reductions, the proposed methods consistently outperform it, particularly in scenarios involving coordinated charging and V2G programs.

As mentioned earlier, approximately 118,000 electric vehicles were active in Ontario in October 2023, and the number of electric vehicles in

Table 4
Total costs for all methods in different scenarios.

Approach	Total cost (thousands of dollars)					
	Type A (by considering the depreciation cost of EVs)			Type B (without considering the depreciation cost of EVs)		
	Scenario 1	Scenario 2	Scenario 3	Scenario 1	Scenario 2	Scenario 3
RA-IGDT	22,746	22,136	21,467	22,288	21,702	20,548
RS-IGDT	20,580	20,057	19,423	20,166	19,659	18,557
Robust	23,486	22,727	21,914	23,452	22,617	21,287
Baseline	21,663	21,082	20,445	21,227	20,694	19,534

Table 6
Total costs for different numbers of active EVs.

Number of EVs	Total cost (k$)		
	Scenario 1	Scenario 2	Scenario 3
118,000	21,663	21,082	20,445
500,000	22,973	22,077	21,106
1,000,000	24,126	22,944	21,774

Table 7
Improvement percentages of total cost with different numbers of active EVs.

Number of EVs	Improvement percentage of total cost	
	From scenario 1 to scenario 2	From scenario 2 to scenario 3
118,000	2.37	2.71
500,000	3.90	4.40
1,000,000	4.90	5.10

Ontario is expected to increase to one million in 2030. Table 6 shows the optimal total costs (without applying uncertainty management methods) for three different possibilities with respect to the number of electric cars (see Fig. 7).

Table 7 presents the percentages of improvement of the total cost when transitioning between scenarios. This table establishes that as the number of electric vehicles increases, moving from the first scenario to the second and third scenarios improves the objective function value. The rate of improvement is higher under the third scenario. The depreciation cost of EV batteries is included in all cases.

The robustness of the results in this study depends on the assumptions made and the flexibility of the coefficients used in the uncertainty modeling methods. The coefficients for the robust method and the IGDT approaches (RS-IGDT and RA-IGDT) are set at specific percentages based on the assumptions and needs of the network. These percentages can vary depending on the operational requirements of the energy hub or the grid operator at acceptable levels of uncertainty. The degree of robustness can be adjusted to fit the conditions of the day being considered (e.g., peak energy demand days, extreme weather events, or geopolitical disruptions). These factors influence how the coefficients are chosen and directly impact the robustness of the results.

The proposed approach guarantees convergence to the global optimum for the given optimization problem due to the use of solvers designed for global optimization. Specifically, the problem was solved using both the BARON and CPLEX solvers within the GAMS software environment. These solvers are known for their capability to handle mixed integer programming (MIP) problems efficiently. The solutions obtained from both solvers were identical, indicating convergence to the global optimum.

6. Conclusion

In this article, the province of Ontario, Canada, was considered as a case study for a large energy hub. Furthermore, we considered all types of power plants available in this province. To deal with the inherent uncertainty of the energy hub, in this article three different methods of dealing with uncertainty were investigated: RA-IGDT, RS-IGDT, and robust method. The uncertainty of the parking lots for electric vehicles was handled using the CVaR method.

According to the results obtained, the coordinated charging of electric vehicles and their participation in the V2G program improve the overall costs of the system. Furthermore, the government of Canada has planned to significantly increase the number of EVs in the next few years. Fortunately, the overall costs of the energy hub decrease significantly when more EVs participate in the V2G program. The government can incentivize the participation of users in the V2G program to further reduce the costs of the energy hub. Note that these results hold even if the depreciation costs of EV batteries are considered in the simulation.

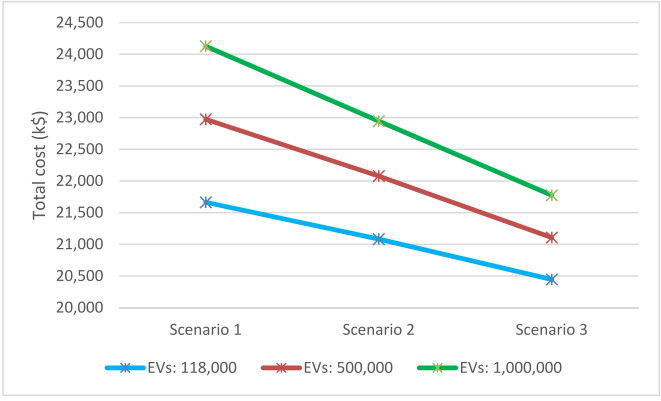

Fig. 7. Total costs on three scenarios for three different numbers of EVs.

This study incorporates a comprehensive uncertainty analysis using RA-IGDT, RS-IGDT, and robust optimization methods to address deviations in energy demands, electricity prices, and renewable energy production. These analyses ensure the robustness and reliability of the proposed energy hub model under various scenarios and operational conditions.

According to the results shown in Table 6, as the number of electric cars within the energy hub increases, the results of the third scenario (Using the V2G mode for EVs, adding thermal and cooling storage units, and performing DRP) prove to be dominant compared to the second scenario (charging EVs in a coordinated manner). After comparing the results of the three discussed solution methods, that is, robust optimization, RA-IGDT, and RS-IGDT, we suggest using the RA-IGDT method for normal conditions because this method considers a confidence margin for uncertain parameters. Therefore, if these parameters are worse than the expectations, the power production plan will not be adversely affected and production can be followed based on the developed plan. However, the RA-IGDT method adheres to the most probable scenarios and does not consider the worst-case situation. Consequently, the robust method is recommended for abnormal conditions in which it is highly probable that the values of uncertain parameters change drastically from expectations.

This article focused on planning for the operations of an energy hub during a 24-h horizon. We believe that monthly and annual planning schedules for an energy hub by applying the methods developed in this article are an attractive research topic. Detailed analysis of the weighting of uncertain parameters in different solution methods is also an inspiring future research direction. Undoubtedly, electric vehicles will play a larger role in energy hubs in the future. As a result, a detailed discussion and analysis of EVs, including the characteristics of various types of EV batteries and the related uncertainties, is an important topic for future research.

The integration of RA-IGDT, RS-IGDT, Robust Optimization, and CVaR methods provides a comprehensive framework for managing uncertainties in energy hub operations. While the primary focus is on the three core methods, CVaR complements the analysis by addressing specific uncertainties related to EV behaviors, enhancing the robustness of the proposed approach. These approaches not only enhance the robustness of energy hub operations, but also provide actionable insights for real-world energy management under uncertainty.

For future work, the focus could shift towards analyzing the operation and performance of specific power plants, designing scenarios that emphasize their role within energy hubs under various uncertainties. Additionally, the methodology applied in this study could be expanded to a larger scale, such as analyzing an entire country, to better understand the dynamics of the energy distribution at a broader level. Another promising direction involves a more detailed investigation of electric vehicles, including different types of electric trucks and buses, to explore their unique charging behaviors and their impact on energy hubs.

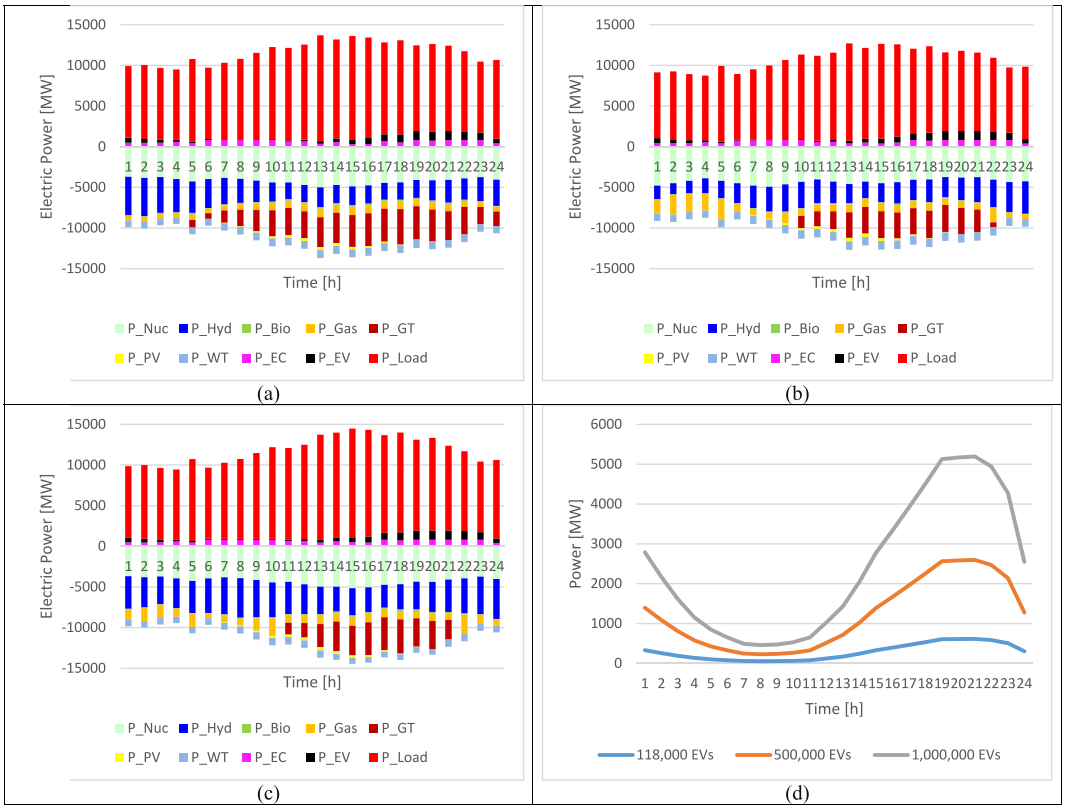

Fig. 1. Optimal electrical power flow under scenario 1: (a) RA-IGDT method, (b) RS-IGDT method, (c) robust method. (d) Uncoordinated charging load of EVs.

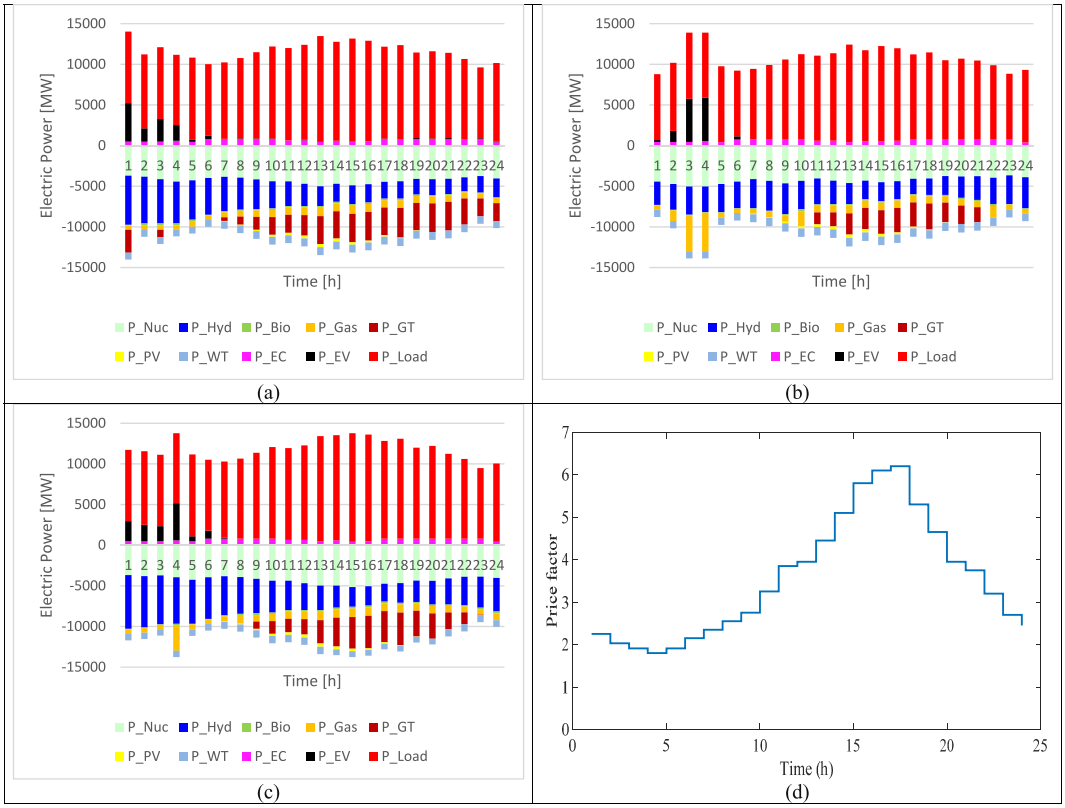

Fig. 2. Optimal electrical power flow under scenario 2: (a) RA-IGDT method, (b) RS-IGDT method, (c) robust method. (d) Price factor defined for daily hours.

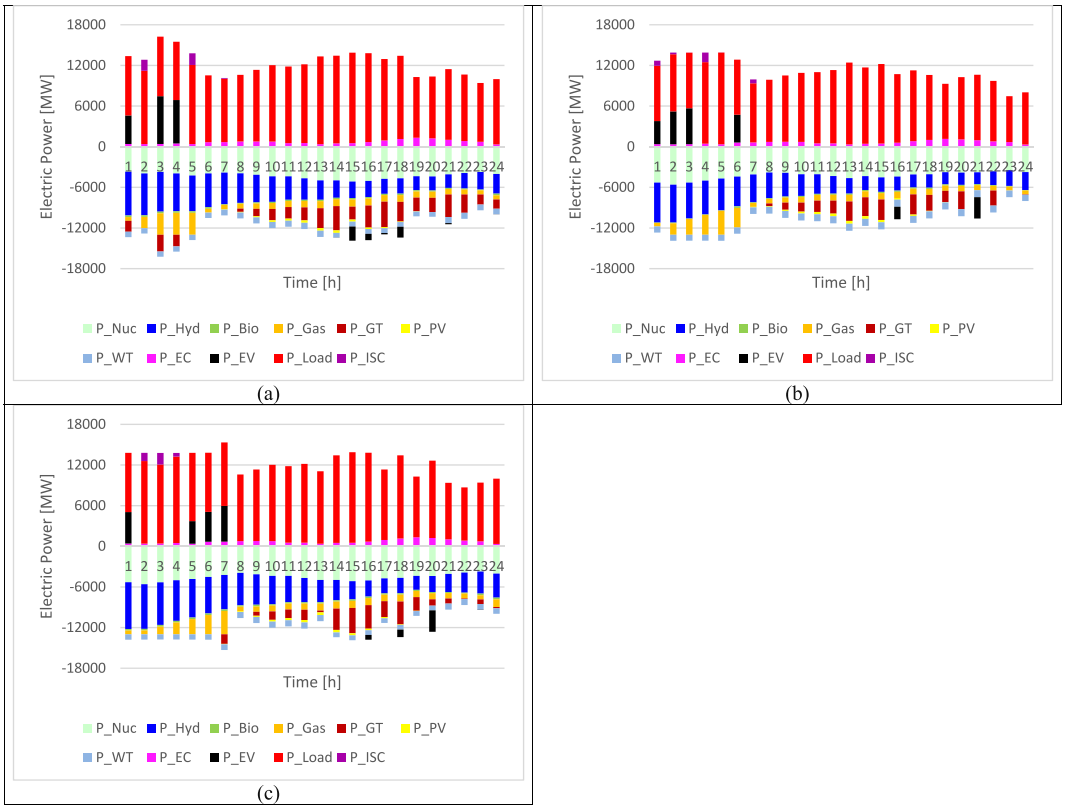

Fig. 3. Optimal electrical power flow under scenario 3: (a) RA-IGDT method, (b) RS-IGDT method, (c) robust method.

Fig. 4. Optimal heating power flow under scenario 1: (a) RA-IGDT method, (b) RS-IGDT method, (c) robust method.

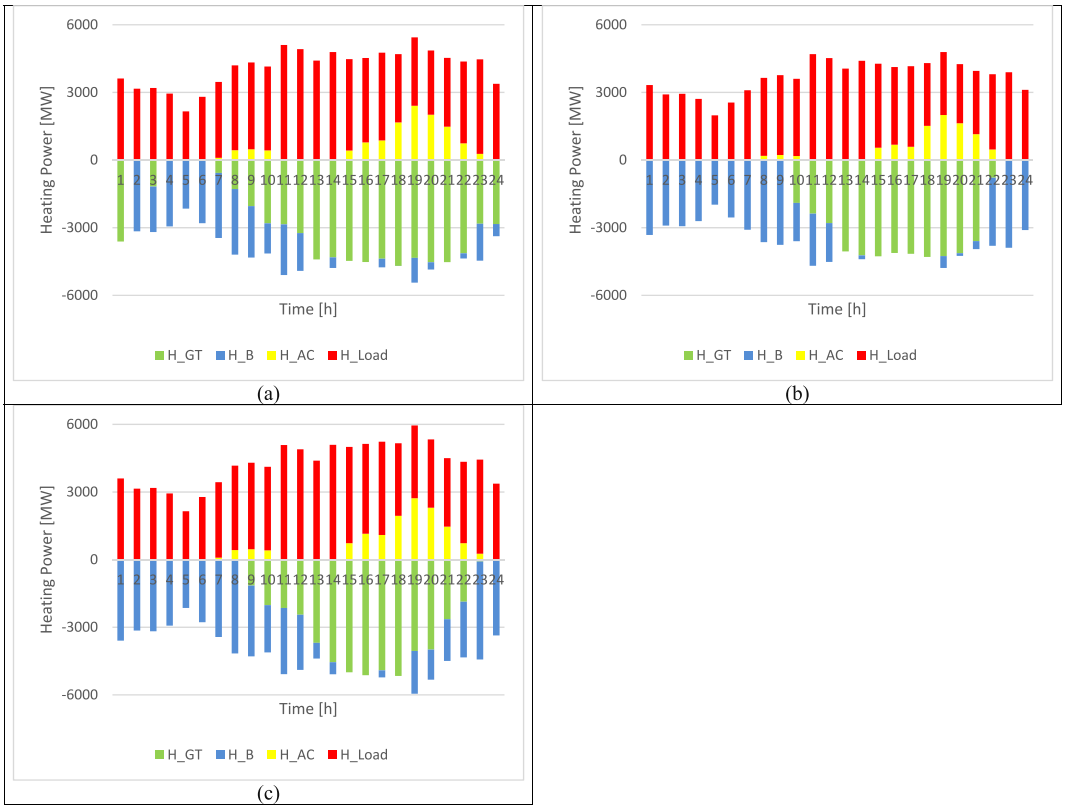

Fig. 5. Optimal heating power flow under scenario 2: (a) RA-IGDT method, (b) RS-IGDT method, (c) robust method.

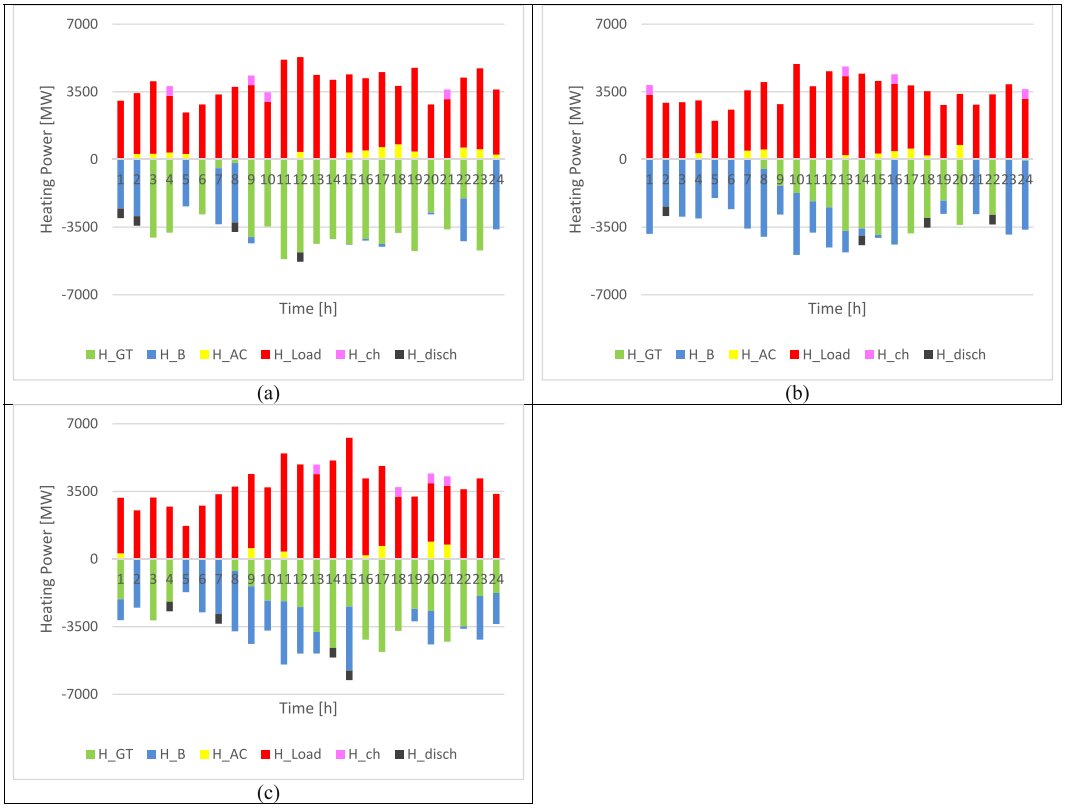

Fig. 6. Optimal heating power flow under scenario 3: (a) RA-IGDT method, (b) RS-IGDT method, (c) robust method.

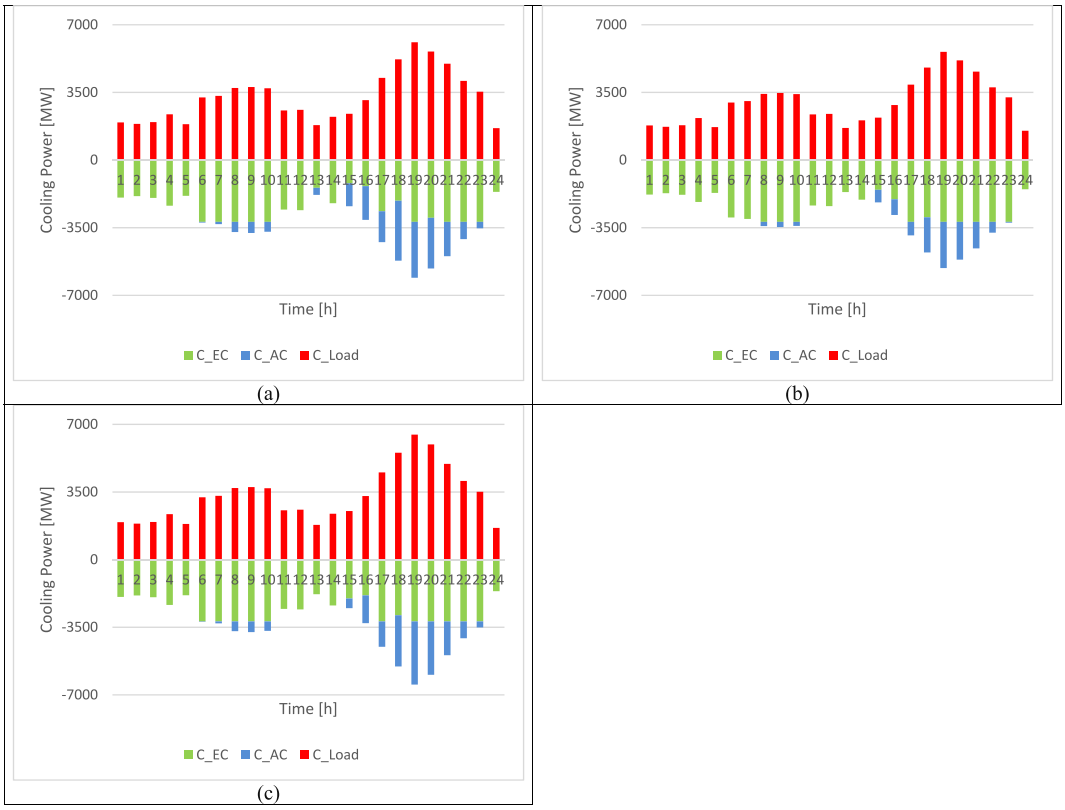

Fig. 7. Optimal cooling power flow under scenario 1: (a) RA-IGDT method, (b) RS-IGDT method, (c) robust method.

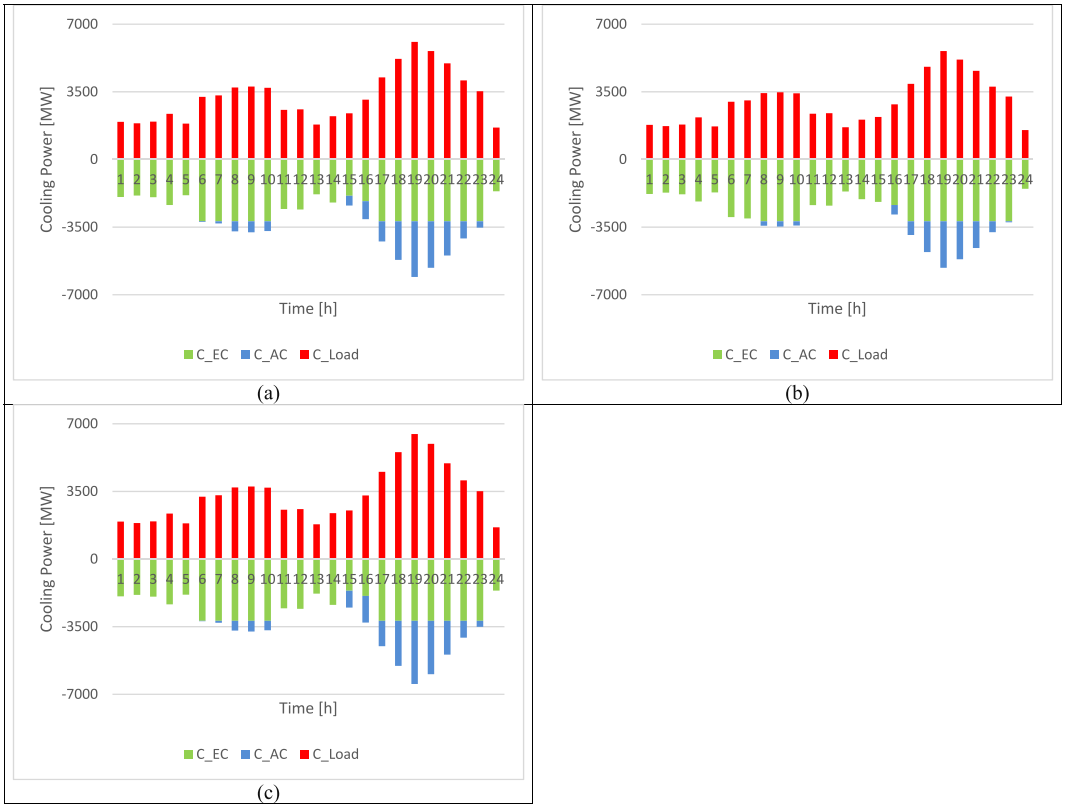

Fig. 8. Optimal cooling power flow under scenario 2: (a) RA-IGDT method, (b) RS-IGDT method, (c) robust method.

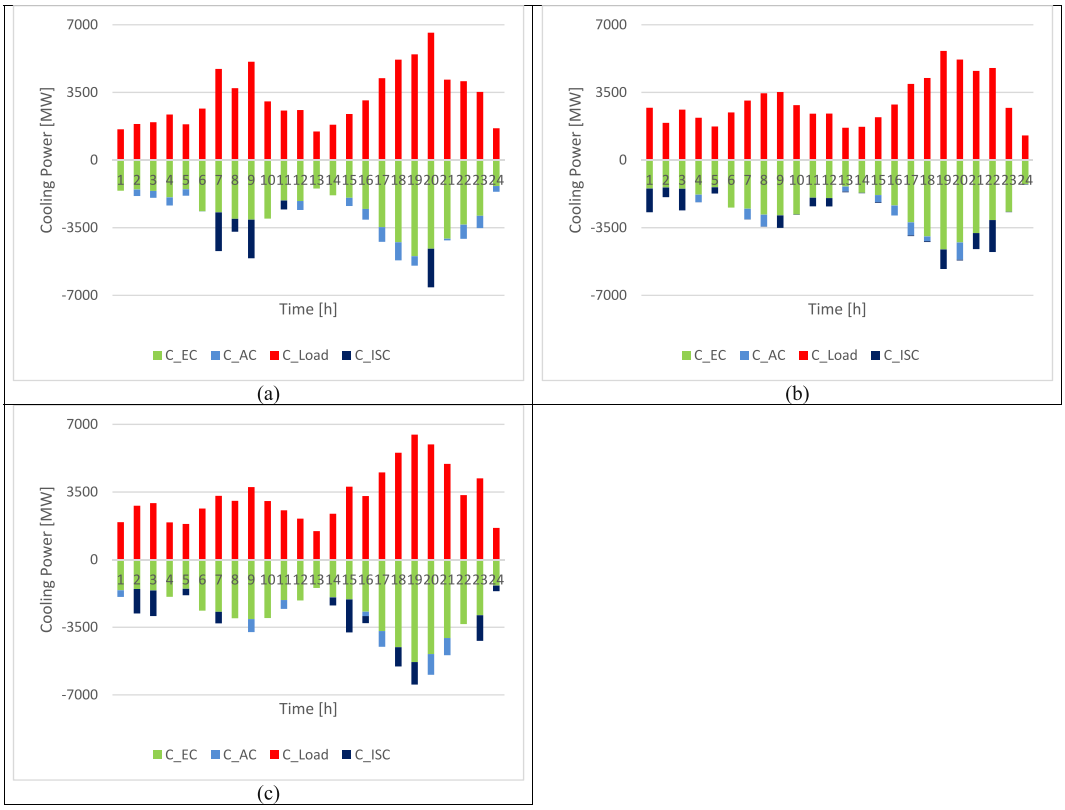

Fig. 9. Optimal cooling power flow under scenario 3: (a) RA-IGDT method, (b) RS-IGDT method, (c) robust method.

CRediT authorship contribution statement

Ahmad Siroos: Writing – original draft, Visualization, Validation, Software, Resources, Methodology, Investigation, Formal analysis, Data curation, Conceptualization. **Hamed Samarghandi:** Writing – review & editing, Validation, Supervision, Project administration, Funding acquisition.

Declaration of competing interest

The authors declare the following financial interests/personal relationships which may be considered as potential competing interests: Dear Professor Henrik Lund,

The authors certify that they have NO affiliations with or involvement in any organization or entity with any financial interest (such as honoraria; educational grants; participation in speakers' bureaus; membership, employment, consultancies, stock ownership, or other equity interest; and expert testimony or patent-licensing arrangements), or non-financial interest (such as personal or professional relationships, affiliations, knowledge or beliefs) in the subject matter or materials discussed in this manuscript.

Acknowledgements

The authors gratefully acknowledge the financial support provided by Canada's "NSERC Discovery Grant [#2017-03743]" and the "Edwards Enhancement Chair in Business Program," which facilitated the completion of this research.

Data availability

Data will be made available on request.

References

[1] Poursmaeil B, Hosseinpour Najmi P, Najafi Ravadanegh S. Interconnected-energy hubs robust energy management and scheduling in the presence of electric vehicles considering uncertainties. J Clean Prod 2021;316:128167. https://doi.org/10.1016/j.jclepro.2021.128167.

[2] Ma T, Wu J, Hao L. Energy flow modeling and optimal operation analysis of the micro energy grid based on energy hub. Energy Convers Manag 2017;133:292–306. https://doi.org/10.1016/j.enconman.2016.12.011.

[3] Kafaei M, Sedighizadeh D, Sedighizadeh M, Fini AS. An IGDT/Scenario based stochastic model for an energy hub considering hydrogen energy and electric vehicles: a case study of Qeshm Island, Iran. Int J Electr Power Energy Syst 2022;135:107477. https://doi.org/10.1016/j.ijepes.2021.107477.

[4] AkbaiZadeh M, Niknam T, Kavousi-Fard A. Adaptive robust optimization for the energy management of the grid-connected energy hubs based on hybrid meta-heuristic algorithm. Energy 2021;235:121171. https://doi.org/10.1016/j.energy.2021.121171.

[5] Han T, Yan Y, Safar B. Optimal integration of CCHP with electric Vehicle parking lots in energy hub. Sustain Energy Technol Assessments 2023;58:103324. https://doi.org/10.1016/j.seta.2023.103324.

[6] Baringo L, Carrión M, Domínguez R. Day-ahead market scheduling considering electric vehicles. In: Baringo L, Carrión M, Domínguez R, editors. Electr. Veh. Renew. Gener. Power Syst. Oper. Plan. Uncertain. Cham: Springer International Publishing; 2023. p. 195–240. https://doi.org/10.1007/978-3-031-09079-0_5.

[7] Zhong J, Li Y, Wu Y, Cao Y, Li Z, Peng Y, Qiao X, Xu Y, Yu Q, Yang X, Li Z, Shahidehpour M. Optimal operation of energy hub: an integrated model combined distributionally robust optimization method with stackelberg game. IEEE Trans Sustain Energy 2023;14:1835–48. https://doi.org/10.1109/TSTE.2023.3252519.

[8] Esrafilian M, Ahmadi R. Energy, environmental and economic assessment of a polygeneration system of local desalination and CCHP. Desalination 2019;454:20–37. https://doi.org/10.1016/j.desal.2018.12.004.

[9] Emrani-Rahaghi P, Hashemi-Dezaki H, Hasankhani A. Optimal stochastic operation of residential energy hubs based on plug-in hybrid electric vehicle uncertainties using two-point estimation method. Sustain Cities Soc 2021;72:103059. https://doi.org/10.1016/j.scs.2021.103059.

[10] Mazidi M, Zakariazadeh A, Jadid S, Siano P. Integrated scheduling of renewable generation and demand response programs in a microgrid. Energy Convers Manag 2014;86:1118–27. https://doi.org/10.1016/j.enconman.2014.06.078.

[11] Farshidian B, Ghahnavieh AR. A comprehensive framework for optimal planning of competing energy hubs based on the game theory. Sustain. Energy Grids Netw. 2021;27:100513. https://doi.org/10.1016/j.segan.2021.100513.

[12] Amir Mansouri S, Javadi MS, Ahmarinejad A, Nematbakhsh E, Zare A, Catalão JPS. A coordinated energy management framework for industrial, residential and

commercial energy hubs considering demand response programs. Sustain Energy Technol Assessments 2021;47:101376. https://doi.org/10.1016/j.seta.2021.101376.
[13] Dini A, Hassankashi A, Pirouzi S, Lehtonen M, Arandian B, Baziar AA. A flexible-reliable operation optimization model of the networked energy hubs with distributed generations, energy storage systems and demand response. Energy 2022;239:121923. https://doi.org/10.1016/j.energy.2021.121923.
[14] Benyaghoob-Sani A, Sedighizadeh M, Sedighizadeh D, Abbasi R. A RA-IGDT model for stochastic optimal operation of a microgrid based on energy hub including cooling and thermal energy storages. Int J Electr Power Energy Syst 2021;131:107092. https://doi.org/10.1016/j.ijepes.2021.107092.
[15] Javadi MS, Anvari-Moghaddam A, Guerrero JM. Optimal scheduling of a multi-carrier energy hub supplemented by battery energy storage systems. In: 2017 IEEE int. Conf. Environ. Electr. Eng. 2017 IEEE Ind. Commer. Power Syst. Eur. EEEIC ICPS Eur.; 2017. p. 1–6. https://doi.org/10.1109/EEEIC.2017.7977520.
[16] Rayati M, Sheikhi A, Ranjbar AM. Applying reinforcement learning method to optimize an Energy Hub operation in the smart grid. In: 2015 IEEE power energy Soc. Innov. Smart grid Technol. Conf. ISGT; 2015. p. 1–5. https://doi.org/10.1109/ISGT.2015.7131906.
[17] Li R, Wei W, Mei S, Hu Q, Wu Q. Participation of an energy hub in electricity and heat distribution markets: an MPEC approach. IEEE Trans Smart Grid 2019;10:3641–53. https://doi.org/10.1109/TSG.2018.2833279.
[18] La Scala M, Vaccaro A, Zobaa AF. A goal programming methodology for multiobjective optimization of distributed energy hubs operation. Appl Therm Eng 2014;71:658–66. https://doi.org/10.1016/j.applthermaleng.2013.10.031.
[19] Dzobo O, Xia X. Optimal operation of smart multi-energy hub systems incorporating energy hub coordination and demand response strategy. J Renew Sustain Energy 2017;9:045501. https://doi.org/10.1063/1.4993046.
[20] Ullah Z, Mokryani G, Campean F, Hu YF. Comprehensive review of VPPs planning, operation and scheduling considering the uncertainties related to renewable energy sources. IET Energy Syst. Integr. 2019;1:147–57. https://doi.org/10.1049/iet-esi.2018.0041.
[21] Shi Y, Zhao Q, Jiao L. Optimum exploitation of multiple energy system using IGDT approach and risk aversion strategy and considering compressed air storage with solar energy. Energy 2024;291:130369. https://doi.org/10.1016/j.energy.2024.130369.
[22] Jasinski M, Najafi A, Homaee O, Kermani M, Tsaousoglou G, Leonowicz Z, Novak T. Operation and planning of energy hubs under uncertainty—a review of mathematical optimization approaches. IEEE Access 2023;11:7208–28. https://doi.org/10.1109/ACCESS.2023.3237649.
[23] Cao Y, Wang Q, Du J, Nojavan S, Jermsittiparsert K, Ghadimi N. Optimal operation of CCHP and renewable generation-based energy hub considering environmental perspective: an epsilon constraint and fuzzy methods. Sustain. Energy Grids Netw. 2019;20:100274. https://doi.org/10.1016/j.segan.2019.100274.
[24] Fang X, Yang Q, Dong W. Fuzzy decision based energy dispatch in offshore industrial microgrid with desalination process and multi-type DGs. Energy 2018;148:744–55. https://doi.org/10.1016/j.energy.2018.01.185.
[25] Lu X, Liu Z, Ma L, Wang L, Zhou K, Feng N. A robust optimization approach for optimal load dispatch of community energy hub. Appl Energy 2020;259:114195. https://doi.org/10.1016/j.apenergy.2019.114195.
[26] Wen P, Xie Y, Huo L, Tohidi A. Optimal and stochastic performance of an energy hub-based microgrid consisting of a solar-powered compressed-air energy storage system and cooling storage system by modified grasshopper optimization algorithm. Int J Hydrogen Energy 2022;47:13351–70. https://doi.org/10.1016/j.ijhydene.2022.02.081.
[27] A CVaR-Robust-Based Multi-Objective Optimization Model for Energy Hub Considering Uncertainty and E-Fuel Energy Storage in Energy and Reserve Markets | IEEE Journals & Magazine | IEEE Xplore, (n.d.). https://ieeexplore.ieee.org/document/9497046 (accessed February 27, 2024).
[28] Mirzaee H, Samarghandi H, Willoughby K. A robust optimization model for green supplier selection and order allocation in a closed-loop supply chain considering cap-and-trade mechanism. Expert Syst Appl 2023;228:120423. https://doi.org/10.1016/j.eswa.2023.120423.
[29] Shams MH, Shahabi M, MansourLakouraj M, Shafie-khah M, Catalão JPS. Adjustable robust optimization approach for two-stage operation of energy hub-based microgrids. Energy 2021;222:119894. https://doi.org/10.1016/j.energy.2021.119894.
[30] Allahvirdizadeh Y, Galvani S, Shayanfar H, Parsa Moghaddam M. Risk-averse scheduling of an energy hub in the presence of correlated uncertain variables considering time of use and real-time pricing-based demand response programs. Energy Sci Eng 2022;10:1343–72. https://doi.org/10.1002/ese3.1104.
[31] Vahid-Pakdel MJ, Nojavan S, Mohammadi-ivatloo B, Zare K. Stochastic optimization of energy hub operation with consideration of thermal energy market and demand response. Energy Convers Manag 2017;145:117–28. https://doi.org/10.1016/j.enconman.2017.04.074.
[32] Heidari A, Mortazavi SS, Bansal RC. Equilibrium state of a price-maker energy hub in a competitive market with price uncertainties. IET Renew Power Gener 2020;14:976–85. https://doi.org/10.1049/iet-rpg.2019.0958.
[33] Zhang X, Yu X, Ye X, Pirouzi S. Economic energy managementof networked flexi-renewable energy hubs according to uncertainty modeling by the unscented transformation method. Energy 2023;278:128054. https://doi.org/10.1016/j.energy.2023.128054.
[34] Akbari E, Mousavi Shabestari SF, Pirouzi S, Jadidoleslam M. Network flexibility regulation by renewable energy hubs using flexibility pricing-based energy management. Renew Energy 2023;206:295–308. https://doi.org/10.1016/j.renene.2023.02.050.
[35] Jokar MR, Shahmoradi S, Mohammed AH, Foong LK, Le BN, Pirouzi S. Stationary and mobile storages-based renewable off-grid system planning considering storage degradation cost based on information-gap decision theory optimization. J Energy Storage 2023;58:106389. https://doi.org/10.1016/j.est.2022.106389.
[36] Piltan G, Pirouzi S, Azarhooshang A, Rezaee Jordehi A, Paeizi A, Ghadamyari M. Storage-integrated virtual power plants for resiliency enhancement of smart distribution systems. J Energy Storage 2022;55:105563. https://doi.org/10.1016/j.est.2022.105563.
[37] Borge-Diez D, García-Moya FJ, Cabrera-Santana P, Rosales-Asensio E. Feasibility analysis of wind and solar powered desalination plants: an application to islands. Sci Total Environ 2021;764:142878. https://doi.org/10.1016/j.scitotenv.2020.142878.
[38] Wang Z, Lin X, Tong N, Li Z, Sun S, Liu C. Optimal planning of a 100% renewable energy island supply system based on the integration of a concentrating solar power plant and desalination units. Int J Electr Power Energy Syst 2020;117:105707. https://doi.org/10.1016/j.ijepes.2019.105707.
[39] Tu T, Rajarathnam GP, Vassallo AM. Synergic integration of desalination and electric vehicle loads with hybrid micro-grid sizing and control: an Island Case Study. Energy Storage 2020;2:e104. https://doi.org/10.1002/est2.104.
[40] Potential for Thermal Water Desalination Using Microgrid and Solar Thermal Field Energy Surpluses in an Isolated Community, Springerprofessional.De (n.d.). https://www.springerprofessional.de/en/potential-for-thermal-water-desalination-using-microgrid-and-sol/17544572 (accessed March 14, 2024).
[41] Luo X, Zhu Y, Liu J, Liu Y. Design and analysis of a combined desalination and standalone CCHP (combined cooling heating and power) system integrating solar energy based on a bi-level optimization model. Sustain Cities Soc 2018;43:166–75. https://doi.org/10.1016/j.scs.2018.08.023.
[42] Kafaei M, Sedighizadeh D, Sedighizadeh M, Sheikhi Fini A. A two-stage IGDT/TPEM model for optimal operation of a smart building: a case study of Gheshm Island, Iran. Therm Sci Eng Prog 2021;24:100955. https://doi.org/10.1016/j.tsep.2021.100955.
[43] Nikmehr N. Distributed robust operational optimization of networked microgrids embedded interconnected energy hubs. Energy 2020;199:117440. https://doi.org/10.1016/j.energy.2020.117440.
[44] Liu J, Chen C, Liu Z, Jermsittiparsert K, Ghadimi N. An IGDT-based risk-involved optimal bidding strategy for hydrogen storage-based intelligent parking lot of electric vehicles. J Energy Storage 2020;27:101057. https://doi.org/10.1016/j.est.2019.101057.
[45] Baringo L, Carrión M, Domínguez R. Mathematical tools. In: Baringo L, Carrión M, Domínguez R, editors. Electr. Veh. Renew. Gener. Power syst. Oper. Plan. Uncertain. Cham: Springer International Publishing; 2023. p. 87–147. https://doi.org/10.1007/978-3-031-09079-0_3.
[46] Ontario Launches Grid Innovation Fund, News.Ontario.Ca (n.d.). https://news.ontario.ca/en/release/1004419/ontario-launches-grid-innovation-fund (accessed June 5, 2024).
[47] C.E.R. Government of Canada. Cer – provincial and territorial energy profiles – Ontario. https://www.cer-rec.gc.ca/en/data-analysis/energy-markets/provincial-territorial-energy-profiles/provincial-territorial-energy-profiles-ontario.html. [Accessed 16 April 2024].
[48] Projected costs of generating electricity 2020 – analysis. IEA; 2020. https://www.iea.org/reports/projected-costs-of-generating-electricity-2020. [Accessed 16 April 2024].
[49] Fact check: Is nuclear energy good for the climate? – DW – 11/29/2021, Dw.Com (n.d.). https://www.dw.com/en/fact-check-is-nuclear-energy-good-for-the-climate/a-59853315 (accessed April 16, 2024)..